

⁶LSCE/IPSL, Gif-sur-Yvette, France

⁷University “Federico II”, Naples, Italy

Received: 14 April 2010 – Accepted: 19 April 2010 – Published: 10 May 2010

Correspondence to: D. Iudicone (iudicone@szn.it)

Published by Copernicus Publications on behalf of the European Geosciences Union.

BGD

7, 3393–3451, 2010

Watermasses and the Southern Ocean carbon cycle

D. Iudicone et al.

Title Page

Abstract

Introduction

Conclusions

References

Tables

Figures

◀

▶

◀

▶

Back

Close

Full Screen / Esc

Printer-friendly Version

Interactive Discussion



Abstract

5 A watermass-based framework is presented for a quantitative understanding of the processes controlling the cycling of carbon in the Southern Ocean. The approach is developed using a model simulation of the global carbon transports within the ocean and with the atmosphere. It is shown how the watermass framework sheds light on the interplay between biology, air-sea gas exchange, and internal ocean transport including diapycnal processes, and the way in which this interplay controls the large-scale ocean-atmosphere carbon exchange.

10 The simulated pre-industrial regional patterns of DIC distribution and the global distribution of the pre-industrial air-sea CO₂ fluxes compare well with other model results and with results from an ocean inversion method. The main differences are found in the Southern Ocean where the model presents a stronger CO₂ outgassing south of the polar front, a result of the upwelling of DIC-rich deep waters into the surface layer. North of the subantarctic front the typical temperature-driven solubility effect produces a net ingassing of CO₂. The biological controls on surface CO₂ fluxes through primary production is generally smaller than the temperature effect on solubility. Novel to this study is also a Lagrangian trajectory analysis of the meridional transport of DIC. The analysis allows to evaluate the contribution of separate branches of the global thermohaline circulation (identified by watermasses) to the vertical distribution of DIC throughout the Southern Ocean and towards the global ocean. The most important new result is that the overturning associated with Subantarctic Mode Waters sustains a northward net transport of DIC (15.7×10^7 mol/s across 30° S). This new finding, which has also relevant implications on the prediction of anthropogenic carbon redistribution, results from the specific mechanism of SAMW formation and its source waters whose consequences on tracer transports are analyzed for the first time in this study.

25

BGD

7, 3393–3451, 2010

Watermasses and the Southern Ocean carbon cycle

D. Iudicone et al.

Title Page

Abstract

Introduction

Conclusions

References

Tables

Figures



Back

Close

Full Screen / Esc

Printer-friendly Version

Interactive Discussion



1 Introduction

In this study we present a new method for understanding the large-scale controls on the Southern Ocean carbon cycle that is rooted in a watermass framework. Watermasses are the phenomenological expression of large-scale ocean dynamical processes, and for this reason they are ubiquitous in characterizing the large-scale circulation structures in the ocean. Not only are watermasses critical to identifying and understanding the processes that maintain the mean structures and circulation patterns, but they will also be of fundamental importance in identifying secular trends in their properties (Bindoff and McDougall, 1994).

The new approach presented here is premised on the assumption that watermasses offer an appropriate unifying framework for understanding the carbon cycle, and this is explored through the use of a three dimensional global model simulation. The watermass approach seeks to unify the relative contributions of ocean circulation and mixing, air-sea gas exchange, and biological processes as they impact the ocean interior as well as the exchange of carbon between the oceanic and atmospheric reservoirs (the climate connection). Research over the last several decades has firmly established that the Southern Ocean serves as a watermass crossroads for the global ocean circulation (e.g., Lumpkin and Speer, 2007 and references therein) as well as for global biogeochemical cycles (Sarmiento et al., 2004; Marinov et al., 2006, and references therein). The analysis of their paths and fate, as well as, of the mass exchanges among them because of transformation processes will be used in this context to characterize their transport capacity for tracers and the transformation of the latter within them or through exchange among them.

The connection between the Southern Ocean and the global ocean circulation is commonly represented as a zonally averaged meridional overturning schematic. This has been used extensively for physical circulation (e.g., Speer et al., 2000) as well as for ocean biogeochemistry and the carbon cycle (e.g., Anderson et al., 2009). Within this framework, however, there are important discrepancies between different scenarios

BGD

7, 3393–3451, 2010

Watermasses and the Southern Ocean carbon cycle

D. Iudicone et al.

Title Page

Abstract

Introduction

Conclusions

References

Tables

Figures



Back

Close

Full Screen / Esc

Printer-friendly Version

Interactive Discussion



that have been proposed that have potentially important implications for the carbon cycle. Since formation and fate of water masses is key to our analysis because of the exchanges connected to those processes, an important distinction that, for example, we wish to highlight here is between the circulation described by the schematics proposed in, e.g., Talley et al. (2003) and those described by Sarmiento et al. (2004) and Anderson et al. (2009) (see Fig. 1). Both schematics agree in many respects, namely that the winds play a critical role in bringing circumpolar deep water (CDW) towards the surface. Although the schematics diverge in a number of important ways, we will focus on two of the important differences here.

First, the schematics differ in terms of the degree of mixing in the ocean interior and the importance of diapycnal transformations below the base of the mixed layer in the consumption of CDW. For Fig. 1a, the internal diapycnal fluxes are thought to be important (e.g., Naveira Garabato et al., 2007; Iudicone et al., 2008a; Zika et al., 2009), whereas in Fig. 1b it is often assumed that the transformations only occur in the mixed layer after CDW has been brought to the surface. Second, the scenarios differ in terms of the formation pathway for Subantarctic Mode Waters (SAMW). For the scenario in Fig. 1a, the subtropical watermass serves as a sizable source for SAMW, with the extension of the western boundary currents of the southern subtropical gyres providing an important contribution. For the schematic in Fig. 1b, the formation of SAMW results largely from transformations driven by air-sea interaction within the surface mixed layer as recently upwelled CDW moves equatorward in the Ekman layer. As yet, there is not a firmly established consensus in the oceanographic literature over which of these scenarios more accurately describes the mean state of the real ocean.

In developing a watermass-driven analysis of the Southern Ocean carbon cycle, it will of course be important to be mindful of these controversies and, interestingly, biogeochemical tracer analysis has the potential to address these controversies. A qualitative link among CO₂ fluxes and water masses was in fact addressed in the study of Mikaloff-Fletcher et al. (2007). In their analysis of the GLODAP (data-based) Key et al. (2004) representation of the pre-anthropogenic carbon cycle, they investigated

BGD

7, 3393–3451, 2010

Watermasses and the Southern Ocean carbon cycle

D. Iudicone et al.

Title Page

Abstract

Introduction

Conclusions

References

Tables

Figures

◀

▶

◀

▶

Back

Close

Full Screen / Esc

Printer-friendly Version

Interactive Discussion



the ΔC_{gasex} tracer originally developed by Gruber et al. (1996). Using ΔC_{gasex} , in their figures the carbon signature of SAMW is one of ingassing for both the Pacific and Atlantic basins, whereas for Antarctic Intermediate Water (AAIW) the signature is one of degassing. This potentially important (and possibly overlooked) result provides first evidence from biogeochemical tracers that the circulation scenario in Fig. 1a is more compatible than that in Fig. 1b, and helps to motivate a more comprehensive and quantitative watermass-based approach.

In addition to an understanding of the ocean interior, we will provide a link to data-based analyses of air-sea gas exchange over the seasonal cycle as well as biological effects. For gas exchange, in addition to a comparison with the climatologies for $p\text{CO}_2$ and CO_2 fluxes from Takahashi et al. (2009), we will also be interested in comparing the seasonal variability in $p\text{CO}_2$ and CO_2 fluxes in the model with what was found in the data-based but mechanistically-oriented study of McNeil et al. (2007). They looked at the relative roles of DIC, alkalinity, temperature, and salinity in controlling seasonal air-sea CO_2 fluxes over the Southern Ocean. Although they considered this for observations where the anthropogenic perturbation is present (whereas it is not in our modeling study), the mechanisms controlling seasonality were the main point of emphasis.

The work here will build on the methods and model simulations (Iudicone et al., 2008a,b and c). In those watermass-based analyses of the ORCA2-LIM model, the pathways and rates of watermass conversion in the Southern Ocean were considered, and referenced to transport across 30°S . It was demonstrated that the Southern Ocean serves as a powerful consumer of the CDW that crosses 30°S from the Atlantic basin, transforming this water into a number of different watermasses both in the interior and at the surface. One of the findings of the Iudicone et al. (2008a) study was that surface water in the AAIW density class is partly maintained by internal ocean conversion of CDW, thus partially masking the CDW upwelling into the mixed layer, and that conversion of SAMW to denser water contributes to the net formation of AAIW. Likewise Iudicone et al. (2008c) revealed that for the model SAMW formation is largely the result

BGD

7, 3393–3451, 2010

Watermasses and the Southern Ocean carbon cycle

D. Iudicone et al.

Title Page

Abstract

Introduction

Conclusions

References

Tables

Figures

◀

▶

◀

▶

Back

Close

Full Screen / Esc

Printer-friendly Version

Interactive Discussion



of cooling of waters of subtropical origin (explaining about 70% of the SAMW formation rate), in broad agreement with McNeil et al. (2001). Given that these watermasses (AAIW and SAMW) are thought to be critical to the uptake of anthropogenic carbon from the atmosphere (Sabine et al., 2004), it is critical to understand the processes that control carbon in this region, in order to understand climate feedbacks.

The main goal of this study is to develop a process-understanding of the large-scale controls on the Southern Ocean carbon cycle. Importantly, the intention is that this understanding is anchored in a watermass framework, and it will proceed in two stages. The first stage will focus on changes that occur at the sea surface, and will seek to understand the processes controlling gas exchanges rates. By focusing on the mean climatological state, it is our intention that the methods developed and presented here can then be applied for the case of climate variability and secular changes in the climate system. The second and third stages of this work will focus on processes within the ocean interior, and will build the novel watermass Eulerian and Lagrangian analyses presented in Ludicone et al. (2008a) and Ludicone et al. (2008c).

2 Methods

The study is based on the detailed, quantitative analysis of the outputs of a global biogeochemical model coupled to a ice-ocean physical model. Due to low interior diapycnal diffusivities in the ocean interior, water volumes have the tendency to conserve properties over long time scales. The ocean is thus structured in a finite number of watermasses, reflecting directly the pattern of the physical processes that determined their formation. Therefore, the understanding of the link between surface fluxes, biogeochemical process in the interior and ocean circulation are more readily identified within a watermass framework. For this reason, we developed a series of quantitative diagnostic tools suited to work in a density space, instead of the standard cartesian space. The numerical methods and the diagnostic tools are presented in the following

BGD

7, 3393–3451, 2010

Watermasses and the Southern Ocean carbon cycle

D. Ludicone et al.

Title Page

Abstract

Introduction

Conclusions

References

Tables

Figures

◀

▶

◀

▶

Back

Close

Full Screen / Esc

Printer-friendly Version

Interactive Discussion



text, while main features of the model module are briefly reported afterwards and in the Appendix.

2.1 Air-sea gas exchange sensitivity

For the first stage of this study, an offline method has been used to provide a measure of the relative impact of different terms that control the seasonal and time-mean fluxes of CO₂ at the air-sea interface. The method consists of a set of separate offline sensitivity experiments derived using output from the control simulation using the two-week means from the climatological (repeating seasonal cycle) fields output from the PISCES model. This method is thus more respectful of some of the nonlinearities that should be expected to contribute to the seasonal cycle in air-sea CO₂ fluxes than what is implicit in the method. The intention is to connect this to the internal watermass transformations and biological processes that can change the distribution of carbon by watermass, which will be consistent with the watermass framework of this study.

The direction and intensity of the modeled air-sea CO₂ flux depends on several parameters. In particular, PISCES computes the air-sea CO₂ flux with the following equation:

$$F = K_W \cdot K_0(p\text{CO}_{2(\text{atm})} - p\text{CO}_{2(\text{sea})}) \quad (1)$$

where K_W is the gas transfer velocity that is largely a function of wind speed and temperature. In PISCES this follows the quadratic relationship of Wanninkhof (1992):

$$K_W = [2.5(0.5246 + 1.6256 \cdot 10^{-2}t + 4.9946 \cdot 10^{-4}t^2) + 0.3 u^2](Sc/660)^{1/2} \quad (2)$$

Sc is the Schmidt number, and K_0 is the solubility coefficient of the carbon dioxide that depends on temperature and salinity of the seawater. In the model this coefficient is computed using the following Eq. Weiss (1974):

$$\ln K_0 = A_1 + A_2(100/T) + A_3 \ln(T/100) + S\%[B_1 + B_2(T/100) + B_3(T/100)^2] \quad (3)$$

BGD

7, 3393–3451, 2010

Watermasses and the Southern Ocean carbon cycle

D. Iudicone et al.

Title Page

Abstract

Introduction

Conclusions

References

Tables

Figures

◀

▶

◀

▶

Back

Close

Full Screen / Esc

Printer-friendly Version

Interactive Discussion



The $p\text{CO}_{2(\text{sea})}$ and the $p\text{CO}_{2(\text{atm})}$ are respectively the partial pressure of the water and the partial pressure of the atmosphere. The difference between the $p\text{CO}_2$ in the surface ocean water and that in the overlying air represents the thermodynamic driving potential for the CO_2 gas transfer across the sea surface (e.g., Feely et al., 2001; Takahashi et al., 2002, 2009). The $p\text{CO}_{2(\text{sea})}$ depends mainly on DIC concentration and the alkalinity of the seawater. As will be seen in Sect. 3, particular attention here is devoted to quantifying the significance of the different model fields that contribute to determining the sign and amplitude of the air-sea CO_2 fluxes. In particular, we are interested in identifying independently the relative contributions of the variability of surface temperature, salinity, DIC, alkalinity, K_0 and K_W . To this end, the seasonal cycle in air-sea CO_2 fluxes was recomputed offline, and the result of this calculation is hereafter referred to as the offline CO_2 flux.

The seasonal and annual mean of air-sea CO_2 flux in the southern hemisphere between 30°S and 80°S are also analyzed in the Sect. 4. A first analysis considered zonally integrated fluxes, but the Southern Ocean circulation and water mass distribution are characterized by fronts that are not perfectly zonal. Therefore, we have also considered the seasonal air-sea flux per each water mass of the surface layer in the Southern Ocean by partitioning the flux into density classes. The surface density varies greatly during the year and, as a consequence, also the association between the front and geographical position. In addition the correspondence between surface and subsurface densities (permanent pycnocline) is maximal in winter. We then used the winter density field for the binning of the surface flux. To classify the water masses we used the neutral density (Jackett and McDougall, 1997) since neutral surfaces constitute a framework that allow for a water mass definition that is consistent for the whole water column of the Southern Ocean. Following Ludicone et al. (2008b) in particular we partitioned the model output into the following classes of water masses (Table 1): TW (Thermocline Water), SAMW (Mode Water), AAIW (Intermediate Water), UCDW (Upper Circumpolar Deep Water) LCDW (Lower Circumpolar Deep Water) and AABW (Antarctic Bottom Water).

Watermasses and the Southern Ocean carbon cycle

D. Ludicone et al.

[Title Page](#)[Abstract](#)[Introduction](#)[Conclusions](#)[References](#)[Tables](#)[Figures](#)[◀](#)[▶](#)[◀](#)[▶](#)[Back](#)[Close](#)[Full Screen / Esc](#)[Printer-friendly Version](#)[Interactive Discussion](#)

Finally, the equation of the flux (Eq. 1) displays its dependency on $p\text{CO}_2(\text{sea})$ which varies with DIC concentration and alkalinity at surface which in turn depend on physical processes such as advection and mixing as well as on biological processes such as remineralization and production. To understand the role of the biological processes on the dynamics of DIC, the biological and physical components of the DIC equation were also considered in the analysis. The equation for the evolution of DIC is:

$$\frac{\partial \text{DIC}}{\partial t} + \mathbf{u} \cdot \nabla \text{DIC} = -\mu^P P - \mu^D D + \lambda_{\text{DOC}}^* \text{DOC} + G^Z Z + G^M M + \lambda_{\text{CaCO}_3}^* \text{CaCO}_3 - P_{\text{CaCO}_3} + \nabla \cdot [k_{\parallel} \nabla_{\parallel} \text{DIC}] + \nabla \cdot [k_{\perp} \nabla_{\perp} \text{DIC}] \quad (4)$$

where: $\mu^P P$ and $\mu^D D$ are the production terms for nanophytoplankton and diatoms; λ_{DOC}^* is the remineralization rate of DOC; $\lambda_{\text{CaCO}_3}^* \text{CaCO}_3$ is the dissolution rate of calcite; P_{CaCO_3} is the production term of calcite; $\mathbf{u} \cdot \nabla \text{DIC}$ is the advection of DIC; $\nabla \cdot [k_{\parallel} \nabla_{\parallel} \text{DIC}] + \nabla \cdot [k_{\perp} \nabla_{\perp} \text{DIC}]$ is the diffusion term i.e., the tendency due to mixing processes can be expressed here in terms of the divergence of isoneutral and dianeutral fluxes (subscript \parallel and \perp , respectively). By analyzing the terms of the equation separately we can thus characterise their contribution on the seasonal evolution of DIC in the surface layer and, indirectly, their contribution to the air-sea CO_2 flux.

2.2 Eulerian analysis of the coupling between physical and biogeochemical processes

The concentration of DIC in the water column is the result of both bio-geochemical processes such as primary production and remineralization and of physical processes such as mixing (Eq. 5). All these sources and sinks are partially fed by the advection of the tracer, i.e., the convergence/divergence of the tracer due to the combination of the tracer concentrations gradients and the oceanic circulation (see Fig. 2). In an isopycnal framework, the latter is evidently the result of physical processes acting to form and subsequently transform the watermass. We thus developed a new quantitative approach

Title Page

Abstract

Introduction

Conclusions

References

Tables

Figures

◀

▶

◀

▶

Back

Close

Full Screen / Esc

Printer-friendly Version

Interactive Discussion



for the analysis of a tracer evolution in a isopycnal framework, which is presented and discussed in Sect. 5.

2.3 Lagrangian analysis

For the third stage of this study, Lagrangian trajectory analysis is introduced to further understand the large-scale circulation controls on the ocean carbon cycle. Lagrangian trajectories were introduced with ocean models by Blanke and Raynaud (1997) as a dynamical diagnostic of the Equatorial Undercurrent in the Pacific Ocean. This method was first applied to ocean biogeochemistry in the study of Radenac et al. (2005). For the current study, particles are released at 30° S, and then their subsequent transformations are referenced to this section. As in Ludicone et al. (2008a), the origin and fate of each water mass has been computed by releasing water parcels at 30° S and stopping the particles when they again cross the 30° S section. We extended the same method to evaluate the pathways by which DIC is transported and redistributed in three dimensions (referenced to crossings at 30° S) by multiplying ϕ_i , the ingoing (outgoing) volume transport per water parcel i , by the DIC value at its initial (final) position. More importantly, the DIC gains/losses were computed by computing the equivalent dilution/concentration values, i.e., as $\Delta\text{DIC} \cdot \phi_i$ where ϕ_i is the volume transport per particle or trajectory (a similar approach has been used to evaluate the buoyancy sinks/losses in Ludicone et al., 2008c). Finally, the transports per trajectory were summed and partitioned into water masses using the density at their final position.

2.4 Model configuration and evaluation

For this study, we use climatologically-varying three-dimensional physical state fields output from a 1500-years spinup of the global coupled ice-ocean model ORCA2-LIM. These fields are used to drive a three dimensional simulation with the PISCES ocean biogeochemistry model (see also the Appendix). Here we shall refer to the model configuration used as ORCA2-LIM-PISCES. The seasonally varying physical state fields

BGD

7, 3393–3451, 2010

Watermasses and the Southern Ocean carbon cycle

D. Ludicone et al.

Title Page

Abstract

Introduction

Conclusions

References

Tables

Figures

◀

▶

◀

▶

Back

Close

Full Screen / Esc

Printer-friendly Version

Interactive Discussion



from year 1500 of the spinup have been used to as input to 5000 years PISCES offline calculation. The physical state fields from this year have been analyzed extensively in the studies of Ludicone et al. (2008a) and Ludicone et al. (2008c). The model circulation and tracers fields correspond well to known features, and in many cases the agreement with observations is excellent. The largest biases in the model of relevance here are an over-production of SAMW in the South Indian Ocean and a weak bottom circulation and overturning (especially in the Indian Ocean).

3 Model evaluation against observed fields and fluxes

We begin with an evaluation of the model results against observations. The physical fields have been validated previously using also tracers simulations such as CFCs, ^3He , and radiocarbon (e.g., Ludicone et al., 2008c; Dutay et al., 2009). We consider a regional decomposition of the air-sea CO_2 fluxes evaluated against the results found in previous modeling studies. This is considered in Fig. 3. For clarity, the figure follows that of Fig. 9 of Mikaloff-Fletcher et al. (2007) (MF07). The comparison includes the inversion results of MF07, the Ocean-Carbon Cycle Model Intercomparison Project (OCMIP) results, and the results from the Community Climate System Model (CCSM) (the same fields that were shown in MF07). Figure 3 reveals a relative consistency between the different estimates over the Southern Ocean, in that there tends to be a region of outgassing poleward of 44°S . However, the meridional structures are distinct in that the ORCA2-LIM-PISCES simulation has a stronger tendency for outgassing over the region south of 58°S relative to the latitude range 44°S – 58°S . The inversion [MF07] found substantial outgassing between 44°S and 58°S , with a mean of $0.37 \pm 0.13 \text{ Pg C/yr}$. We find that the air-sea CO_2 flux at these latitudes is 0.11 Pg C/yr . In the mid-latitudes of the Southern Hemisphere (18°S to 44°S), the inversion gives an uptake of CO_2 with a mean of $0.68 \pm 0.13 \text{ Pg C/yr}$. In the same latitudinal band ORCA2-LIM-PISCES gives an uptake of 0.64 Pg C/yr . Therefore, integrating over the entire Southern Ocean gives about the same outgassing in both the

Watermasses and the Southern Ocean carbon cycle

D. Ludicone et al.

Title Page

Abstract

Introduction

Conclusions

References

Tables

Figures

◀

▶

◀

▶

Back

Close

Full Screen / Esc

Printer-friendly Version

Interactive Discussion



inversion and the ORCA2-LIM-PISCES simulation. A closer look to the MF07 inversion (discussed below) shows that the partitioning into high and mid-latitudes values in the Southern Ocean is possibly not completely robust, given the lack of in situ data in these regions.

5 The global geographical pattern is coherent between the inversion of natural air-sea fluxes of MF07 (see also Gruber et al., 2009) and the modelled fluxes (presented in Fig. 4). The large differences in the Southern Ocean regional patterns will be further discussed in the following section. A further comparison between total air-sea fluxes of Takahashi et al. (2009) and the modelled fluxes (not shown) illustrated that the general
10 modelled pattern is very well reproduced, i.e., the two fields have similar magnitude and good locations of regions with intense sources and sinks, especially in the Southern Ocean. Nevertheless it should be emphasized that the Takahashi et al. (2009) flux climatology also includes an anthropogenic component which limits any detailed comparison.

15 As a second step in evaluating the modeled carbon cycle against observations, we consider next (in Fig. 5) the annual mean distribution of DIC concentrations across 30° S. The data product used here is from the Global Ocean Data Analysis Project (GLODAP) presented in Key et al. (2004). This choice of latitude is consistent with the reference latitude used in the analysis of Ludicone et al. (2008c), and it
20 is an appropriate reference latitude for identifying the large-scale controls on carbon cycling over the entire Southern Ocean. The model is consistent with the data product in producing relatively high DIC concentrations in the deep Pacific Ocean and relatively low DIC concentrations in the Indian Ocean. For the Atlantic, DIC concentrations are intermediate, with a local maximum in the DIC core for both the model and the data
25 product.

As a third evaluation exercise, we next consider the distribution of zonally averaged DIC concentrations and alkalinity in Fig. 6 as a function of latitude and depth. The model has a bias towards high DIC concentrations in the deep ocean, which result in vertical gradients over the entire water column that are too large by as much as 50%.

Watermasses and the Southern Ocean carbon cycle

D. Ludicone et al.

Title Page

Abstract

Introduction

Conclusions

References

Tables

Figures



Back

Close

Full Screen / Esc

Printer-friendly Version

Interactive Discussion



The opposite holds for alkalinity, where the model underestimates the amplitude of the vertical gradients over the entire water column.

4 A water mass analysis of the Southern Ocean CO₂ flux

4.1 The Southern Ocean air-sea CO₂ flux in a density framework

5 The Southern Ocean is a source of CO₂ to the atmosphere for ORCA2-LIM-PISCES (Fig. 4) and MF07. The difference is in the latitudinal distribution of the outgassing. In ORCA2-LIM-PISCES the stronger outgassing can be seen south of 58° S while for the data inversion (MF07) and for other models (Moore et al., 2004) it is located between 44° S and 58° S. We will inspect here these patterns in the following.

10 The separation between regions of outgassing and ingassing is expected to be strongly related to the separation between regions where the water masses upwell and downwell. As was pointed out by Sloyan and Rintoul (2001), commonly used modern schematics of the overturning circulation in the Southern Ocean are qualitatively similar in their main features to the schematic presented by Sverdrup and Deacon in 15 the 1930s (e.g., Sverdrup et al., 1942). The relationship between the overturning circulation and local biogeochemical cycles is crucially linked to the surface expression of the overturning, i.e., the complex ACC frontal system. This is defined as a band of large horizontal tracer gradients that are often associated with intense surface currents. The relationship between water masses boundaries and main currents is not 20 straightforward because of the complex combination of barotropic and baroclinic components of the flow as well as the presence of a significant residual eddy transport (e.g., see Pollard et al., 2002, and Ito et al., 2005, for a discussion). The first implication is that we should expect that the DIC and air-sea fluxes are strongly linked to the frontal system and thus to the water mass distribution (which can be classified using 25 density, for instance). In particular, since the equilibration time for of CO₂ in the mixed layer is about one year, we should expect that the upwelling of DIC-rich CDW and the

BGD

7, 3393–3451, 2010

Watermasses and the Southern Ocean carbon cycle

D. Iudicone et al.

Title Page

Abstract

Introduction

Conclusions

References

Tables

Figures

◀

▶

◀

▶

Back

Close

Full Screen / Esc

Printer-friendly Version

Interactive Discussion



outgassing of CO₂ to the atmosphere should roughly correspond. This simple consideration makes the result of the inversion in MF07 quite surprising, since there is little correlation between the upwelling region of CDW, south of the PF, with the maximum of the outgassing, further north while in the model they are well in agreement (Fig. 4).

5 When interpreting the results from the ocean inversion it is important to keep in mind that basically, for clear limits in the in situ data availability, it has been obtained optimizing fluxes for 33 big ocean regions, and inside those regions the fluxes are forced to follow Takahashi et al. (2002).

10 When considering the relationship between frontal structures and CO₂ fluxes in more detail, it is important to account for the fact that frontal structures are not purely zonal in their orientation. Thus zonal averaging of oceanographic properties over the Southern Ocean tends to introduce spurious mixing of these properties across frontal structures. It is for this reason that the relationship between CO₂ fluxes and dynamical structures is most appropriately addressed through use of a density framework. Given our main
15 goal of connecting fluxes and biology to the ocean interior DIC distribution, we consider the fluxes as a function of surface densities. This is done by taking the winter surface density distribution as a function of latitude and longitude, and maintaining this distribution to be a static reference frame over the full extent of the seasonal cycle. The intention here is to connect the surface CO₂ fluxes to the winter position of isopycnal
20 surface outcrops, which is directly connected with the 3-D frontal structures. Finally, in order to gain a deeper understanding of the mechanisms producing the pattern of air-sea fluxes, we move to a description of the seasonal cycle instead of discussing the annual mean.

4.2 The Southern Ocean air-sea CO₂ seasonal cycle

25 The seasonally varying integrated CO₂ fluxes are shown as a function of density as solid black lines in Fig. 7a for austral winter, Fig. 7b for austral spring, Fig. 7c for austral summer, and Fig. 7d for austral autumn. The CO₂ fluxes integrated over density classes are listed in Tables 2 and 3. A net separation among the TW and SAMW and

BGD

7, 3393–3451, 2010

Watermasses and the Southern Ocean carbon cycle

D. Iudicone et al.

Title Page

Abstract

Introduction

Conclusions

References

Tables

Figures

◀

▶

◀

▶

Back

Close

Full Screen / Esc

Printer-friendly Version

Interactive Discussion



the AAIW and CDW watermasses is clearly evident. The SAMW is the main water mass that absorbs CO₂ from the atmosphere and indeed an ingassing during winter, spring and fall occurs (Fig. 7). The AAIW is a source of CO₂ for the atmosphere, throughout the year. CDW and AABW also provide sources of CO₂ for the atmosphere all over the year.

In terms of contributions to the net flux over the Southern Ocean, however, SAMW and AAIW dominate due to their large areal extent and for being less affected by the ice cover. As it will be seen in the analysis that follows, the air-sea CO₂ fluxes associated with SAMW are in agreement with what was found in the analysis of McNeil et al. (2007). The model results here indicate that SAMW fluxes reflect lateral mixing of TW, and the degree to which TW cools while moving poleward in the Sub-Antarctic Zone (SAZ). The strong model outgassing south of 58° S is consistent with the distribution of the Southern Ocean fronts and with the strong upwelling of water with high DIC concentrations south of the Polar Front. Importantly, the outgassing in the region of AAIW densities, which acts as a bridge between the CDW contribution to upwelling and the SAMW formation region, is due to CDW by vertical and lateral mixing, as described in Sect. 5.

The geographical distribution of air-sea fluxes is shown in Fig. 8. North of 50° S (in the SAZ), it is clear that the wintertime flux of CO₂ is negative. This is also in agreement with Mikaloff-Fletcher et al. (2007), even if in our model the strong outgassing is shifted to the south relative to what is found at those latitudes (as previously seen), and as a consequence the upwelling of DIC is south.

The contour line 27.2 γ separates the Mode Waters and the Intermediate Water respectively north and south of this density range and roughly corresponds to the SAF in the model, which in turn, corresponds well with the mean position of the SAF from data analysis. Figure 8 shows that the outgassing is restricted south of 27.2 γ , becoming stronger south of the SAF. This front and the PF are also located south of this band in the domain of the AAIW. North of 27.2 γ , the flux becomes negative with the stronger ingassing in the domain of SAMW.

BGD

7, 3393–3451, 2010

Watermasses and the Southern Ocean carbon cycle

D. Iudicone et al.

Title Page

Abstract

Introduction

Conclusions

References

Tables

Figures

◀

▶

◀

▶

Back

Close

Full Screen / Esc

Printer-friendly Version

Interactive Discussion



**Watermasses and the
Southern Ocean
carbon cycle**D. Iudicone et al.

[Title Page](#)[Abstract](#)[Introduction](#)[Conclusions](#)[References](#)[Tables](#)[Figures](#)[◀](#)[▶](#)[◀](#)[▶](#)[Back](#)[Close](#)[Full Screen / Esc](#)[Printer-friendly Version](#)[Interactive Discussion](#)

As a first qualitative analysis, we observe that this distribution is also consistent with the distribution of the surface DIC concentrations (Fig. 8). This is also consistent with the results from an empirical estimate of the contemporary Southern Ocean flux (McNeil et al., 2007), where analysing the DIC distributions in the surface ocean, they found that the PF is a distinctive marker between DIC-rich water to the south and more DIC-depleted water to the north. In fact, the seasonal cycle of surface DIC in the model resembles very closely the estimates presented in McNeil et al. (2007) (see their Fig. 5). In particular, the maximum winter values are in the Weddell Sea and neighbouring regions as well as along the coast of Antarctica west of the Ross Sea. West of the Ross Sea, a region of maximum DIC concentrations is separated from the Antarctic continent in both the model and in situ estimates. The main mismatch is observed in the Pacific sector of the Southern Ocean, where the model underestimates the winter concentrations. In summer, for both cases a rather homogeneous band of high DIC concentrations characterises the region south of the SAF, with a local maximum along the coast of the Weddell Sea. A more quantitative correspondance of the seasonal cycle in DIC concentrations and the air-sea CO₂ fluxes will be considered in the next section.

4.3 The physical and biological processes in the seasonal cycle of air-sea CO₂ fluxes

Prior to McNeil et al. (2007), other studies (e.g., Takahashi et al., 1993, and Takahashi et al., 2002) had distinguished the effects of biology and temperature on $p\text{CO}_2$ variations by removing the temperature effect from the measured $p\text{CO}_2$. The resulting changes gave an approximation of the net effect of biology. In addition to the a net utilization of DIC, the biological effect also drives a small net alkalinity change due to carbonate production and nitrate utilization, air-sea exchange of CO₂ and an addition of CO₂ and alkalinity associated with the vertical mixing of subsurface waters. McNeil

et al. (2007) extended this work for the Southern Ocean, making use of the tremendous increase in data density made available through the 1990s and 2000s.

Here these factors are quantitatively addressed separately by investigating the role of the different terms in the CO₂ fluxes and, then, by specifically evaluating the seasonal cycle in DIC concentrations. For models, the linear approach of Takahashi et al. (1993) is usually justified by arguing that perturbations are small. For modeling studies of interannual variability, this method is typically performed on output from a single run. First, the different terms in the CO₂ flux were evaluated separately (see the section on Methods). Figure 7, in addition to the zonally seasonal air-sea CO₂ flux, also shows the air-sea CO₂ fluxes computed removing, respectively: the DIC effect (herein referred as CO₂flux-DIC), the temperature effect (CO₂flux-T), the solubility effect (CO₂flux-K0), the alkalinity effect (CO₂flux-alk), the salinity effect (CO₂flux-sal) and the Kw (gas transfer velocity) effect (CO₂flux-Kw). The sensitivity to DIC and temperature in the seasonal mean of the air-sea CO₂ flux for each water mass is summarized in Tables 2 and 3 while their geographical distributions are presented in Fig. 9. In general, the most important factors determining the seasonal cycle of the air-sea CO₂ flux are the DIC concentrations, the temperature, and the solubility, with solubility being closely related to the temperature. The impact of alkalinity is significant only in some regions.

For the case of TW, the controlling influence of temperature persists through the year. The temperature control is stronger and its effect is to increase the flux toward the atmosphere in summer and to increase the flux toward the ocean in winter. For SAMW, the temperature control on CO₂ fluxes is effective throughout the year, although in fall DIC concentrations are dominant. In summer the effect of temperature causes a flux toward the atmosphere and this effect is not contrasted efficiently from the impact of DIC variability. In winter, cooling increases the flux of CO₂ into the ocean while the DIC effect acts in the opposite sense. Gloor et al. (2003) assert that there is little net air-sea heat flux south of 50° S, so any solubility driven CO₂ flux is small (Mikaloff-Fletcher et al., 2007). This is in strong agreement with the conclusion from McNeil et al. (2007), where it was shown that strong winter cooling lowers $p\text{CO}_2$ in the SAZ. In

BGD

7, 3393–3451, 2010

Watermasses and the Southern Ocean carbon cycle

D. Iudicone et al.

Title Page

Abstract

Introduction

Conclusions

References

Tables

Figures

◀

▶

◀

▶

Back

Close

Full Screen / Esc

Printer-friendly Version

Interactive Discussion



ORCA2-LIM-PISCES, south of 50° S in the region of Intermediate, Deep and Bottom water masses, the DIC effect prevails over the temperature effect. The winter air-sea CO₂ flux for AAIW is characterized by a change from temperature dependence to DIC dependence and a change from a negative CO₂ flux to a positive CO₂ flux (also Tables 2 and 3). In summer, the flux is positive since temperature and alkalinity overcome the effect of DIC. In winter the effect of DIC drives a strong positive flux and its effect prevails over the temperature effect. The air-sea CO₂ flux in the CDW depends on DIC for the entire year, even if in summer the temperature and alkalinity mitigates the DIC effect. Finally the AABW also depends exclusively on DIC.

4.3.1 The physical and biological processes in the seasonal cycle of the surface DIC

In ORCA2-LIM-PISCES, the DIC evolution depends on different factors that can be summarized as follows: a production term that represents the biological consumption of DIC in the surface ocean, a remineralization term representing a source of reconverted inorganic carbon by the heterotrophic organisms, and dissolution and production of calcite that subtracts or adds DIC. All these terms can be grouped as biological/chemical effects (see Sect. 2 on Methods). The other factors influencing the ocean distribution of DIC are the diffusion terms representing the tendency due to mixing processes in both three directions, the advection terms (also both three directions), and of course the air-sea CO₂ flux. According to Murnane et al. (1999) and Mikaloff-Fletcher et al. (2007), the uptake in the north regions of the Southern Ocean is likely driven by the combination of an efficient biological pump and cooling surface of waters that are transported southward by the Ekman circulation. The ORCA2-LIM-PISCES results suggest that for the SAMW the CO₂ flux is mainly driven by the temperature effect (producing a negative flux in winter, fall, and spring, and a positive flux in summer) and, more generally, the effect of seasonal temperature variations north of the SAF. In fact, surface DIC concentrations for SAMW densities (Fig. 10b) decrease in summer due to the effect of the production term and the outgassing flux of CO₂. In fall and winter DIC concentrations

Watermasses and the Southern Ocean carbon cycle

D. Iudicone et al.

Title Page

Abstract

Introduction

Conclusions

References

Tables

Figures



Back

Close

Full Screen / Esc

Printer-friendly Version

Interactive Discussion



in the surface layer increase. In fall this increase depends on the ingassing CO_2 flux, the vertical advection and remineralization term. In winter its increase is due to the sum of the ingassing CO_2 flux, vertical diffusion, and remineralization.

For AAIW (Fig. 10c) the concentration of DIC in the surface layer decreases during the first part of summer, due to the combined effects of the production term, the vertical advection term, and the air-sea CO_2 flux, while the increase in DIC concentrations in fall and winter depends predominantly on vertical diffusion. Although in Fall the DIC concentrations increase, they are still low, causing an ingassing flux of CO_2 . This negative flux and the vertical diffusivity are the main factors that determine the increase of DIC concentrations in the surface layer. DIC is instead the main driver of the outgassing in winter. This increase is thus due to the entrainment of a deep water-mass rich in DIC. The surface DIC concentrations reach their minimum expression in summer, and subsequently increase in fall before reaching its highest values in winter. When the DIC concentrations decrease in spring, this is again due to the production term, the vertical advection term and the CO_2 flux. Note that while in spring and summer the surface concentrations of DIC decrease, the CO_2 flux is still positive due to the temperature and the alkalinity effects that act to oppose the effect of DIC. Finally, according to Murnane et al. (1999), in the region of outgassing, a substantial fraction of upwelled DIC can escape into the atmosphere, as the rate of removal of DIC by biology at the surface is slow and inefficient. In our analysis, production is the most important term that drives the decrease in DIC concentrations in the surface layer in spring and summer. This decrease lowers the intensity of the CO_2 outgassing but it is not enough to drive an ingassing, as during these seasons the effect of temperature opposes the effect of DIC concentrations.

The UCDW and LCDW density classes are sources of CO_2 throughout the year. The seasonal variations in air-sea CO_2 fluxes for these waters have a strong DIC contribution. Nevertheless seasonal alkalinity variations are also important, especially for the UCDW. In summer and spring the effect of DIC is to reduce the positive flux, with concentrations being lowest in summer due to the production term, the advection term and

BGD

7, 3393–3451, 2010

Watermasses and the Southern Ocean carbon cycle

D. Iudicone et al.

Title Page

Abstract

Introduction

Conclusions

References

Tables

Figures

◀

▶

◀

▶

Back

Close

Full Screen / Esc

Printer-friendly Version

Interactive Discussion



the CO₂ flux term. In fact, the concentration of surface DIC in the UCDW (Fig. 10d) increase from the middle of summer until winter mainly due to the vertical diffusion term while its decrease is due to the production term and the vertical advection term plus the CO₂ flux. The annual trend of surface DIC in the surface layer in the LCDW (Fig. 8e) is similar to that of the UCDW. The difference is that the increase of DIC in summer and fall depends mainly on the vertical advection term, while in winter again the vertical diffusion term is the most important term.

For AABW, the seasonal variations in air-sea CO₂ fluxes are largely dominated by seasonal variations in DIC concentrations. The increase of DIC in winter is due to the vertical advection that brings DIC at the surface layer while the vertical diffusivity brings down the DIC from the surface layer. The DIC in the surface layer (Fig. 10f) increases in summer and mid-fall due to the vertical advection term that opposes, in this case, the vertical diffusion term that acts to decrease the surface DIC. From fall to winter the vertical advection term and the vertical diffusion term almost compensate each other, and in spring the production term, together with the vertical advection and the CO₂ flux, determines the decrease of DIC in the surface layer.

5 The DIC evolution and the role of the THC

In the previous section, the influence of surface ocean properties on surface flux CO₂ were characterised and discussed. Since these *properties* depend on three-dimensional processes maintaining the distribution of watermasses, the question arises as to how the carbon cycle is related to the three-dimensional circulation of the ocean. The relationship between the carbon cycle and the thermohaline circulation is characterised first via the quantification of the terms that act on DIC evolution per water mass and, secondly, via the definition of the main water-mass pathways and of the associated DIC gain/loss. This latter analysis has been performed using, first, a novel quantitative approach to the quantitative analysis of the DIC budget per water mass,

BGD

7, 3393–3451, 2010

Watermasses and the Southern Ocean carbon cycle

D. Iudicone et al.

Title Page

Abstract

Introduction

Conclusions

References

Tables

Figures

◀

▶

◀

▶

Back

Close

Full Screen / Esc

Printer-friendly Version

Interactive Discussion



and, secondly, a quantitative Lagrangian tool that allows us to follow the water-masses and the associated evolution of tracer concentrations.

5.1 The DIC evolution per each water mass

5.1.1 Theory

5 Here we extend the *classical* water mass diagnostics of the impact of physical terms on the diapycnal fluxes (initiated by Walin, 1982) to derive a tool for the quantitative analysis of factors (sources/sinks) that determine a tracer 3-D distribution and the role of the physics of the overturning in the advection of the tracer, which is in balance with the sinks/sources (see Fig. 2). More specifically, as starting point we will use the
 10 generalized approach presented in Ludicone et al. (2008b).

Assume that a tracer with concentration per volume C is transported by the flow and it is *active*, i.e., it has sources and sinks π_C and undergoes the effect of diffusion d_C such has that its time evolution is:

$$\frac{DC}{Dt} \equiv \frac{\partial C}{\partial t} + \mathbf{u} \cdot \nabla C = d_C + \pi_C. \quad (5)$$

15 Assuming incompressibility and invoking Gauss' theorem, we can rewrite the evolution of C in the volume V_Y (see Fig. 11) as

$$\int_{V_Y} \frac{\partial C}{\partial t} dv = \int_{V_Y} -\mathbf{u} \cdot \nabla C dv + \int_{V_Y} d_C dv + \int_{V_Y} \pi_C dv = \int_{S_Y} \mathbf{C} \mathbf{u} \cdot \mathbf{n} ds + \int_{V_{S_Y}} \mathbf{C} \mathbf{u} \cdot \mathbf{n} ds \quad (6)$$

$$+ \int_{OS_Y} \phi_a ds + \int_{V_Y} d_C dv + \int_{V_Y} \pi_C dv = -\Phi_Y - \Psi_Y - A_Y + \Sigma_Y + \Pi_Y.$$

20 where the first term is the transport across the isopycnal surface, the second term is the transport at the boundary, the third term is the air-sea flux of the tracer C , the fourth term represents the net effect of the diffusion on the tracer (rewritten using an application of

BGD

7, 3393–3451, 2010

Watermasses and the Southern Ocean carbon cycle

D. Ludicone et al.

Title Page

Abstract

Introduction

Conclusions

References

Tables

Figures

◀

▶

◀

▶

Back

Close

Full Screen / Esc

Printer-friendly Version

Interactive Discussion



Gauss theorem to term) and the last one is the volume integral of source and sinks on the isoneutral layer.

Extending the results in Ludicone et al. (2008b), we now express explicitly the dia-neutral transport of the tracer Φ_γ in terms of the ocean physics, i.e., the processes that act on transforming watermasses, here divided into mixing processes (d_γ) and boundary forcing (f_γ). Defining $\omega_\gamma = (\nabla_\perp \gamma)^{-1}$ as the dianeutral velocity across the moving S_γ , the transport of C per unit surface across a neutral density surface is given by

$$\phi_\gamma = C\omega_\gamma = C(d_\gamma + f_\gamma)(\nabla_\perp \gamma)^{-1}. \quad (7)$$

The total tracer flux Φ_γ across the S_γ is thus

$$\Phi_\gamma = \int_{S_\gamma} C(d_\gamma + f_\gamma)(\nabla_\perp \gamma)^{-1} ds = \underbrace{\frac{\partial}{\partial \gamma} \int_{V_\gamma} C d_\gamma dv}_{10} + \underbrace{\frac{\partial}{\partial \gamma} \int_{V_\gamma} C f_\gamma dv}_{10} \quad (8)$$

where the latter passage was made making use of a generalized form of Leibnitz's theorem. All the terms in Eq. (8) can be easily estimated using the tendency terms for temperature and salinity (d_γ and f_γ ; see Ludicone et al., 2008b) and the tracer field C . Assuming stationarity, the integration of Eq. (7) from the South Pole to a latitude $\theta = \Theta$ gives:

$$\Psi_\gamma(\Theta) \sim \Phi_\gamma(\Theta) - A_\gamma(\Theta) + \Sigma_\gamma(\Theta) + \Pi_\gamma(\Theta). \quad (9)$$

Therefore, combining Eqs. (7) and (8), $\Psi_\gamma(\Theta)$, the northward transport across the line of latitude $\theta = \Theta$ of the tracer by water masses denser than γ , can be expressed in terms of the total diapycnal tracer transport down across γ south of $\theta = \Theta$ and the net effect of the the sources and sinks of the tracer. Equation (8) thus allows one to link the tracer evolution to the ocean physics in a simple and elegant way. In steady state, this in fact correspond to a *generalisation* of generalised meridional streamfunction of Greatbatch and Zhai (2007); see also Marsh et al. (2000); Ludicone et al. (2008b).

BGD

7, 3393–3451, 2010

Watermasses and the Southern Ocean carbon cycle

D. Ludicone et al.

Title Page

Abstract

Introduction

Conclusions

References

Tables

Figures

◀

▶

◀

▶

Back

Close

Full Screen / Esc

Printer-friendly Version

Interactive Discussion



5.1.2 The overturning and the DIC redistribution

In Fig. 12, the diapycnal transports per single physical process are reported from Ludicone et al. (2008a). Using DIC as a tracer in Eq. 8, the role of the physics of overturning in the Southern Ocean on DIC transport (i.e., the transport of DIC due to diapycnal processes) is evaluated quantitatively by computing $\Phi_V(\Theta=30^\circ\text{S})$ (see Fig. 13). In fact, for the case of DIC, geographical variations are small ($\sim 1\text{--}10\%$) and thereby $\Phi_V(\Theta=30^\circ\text{S})$ is roughly proportional to the volume transport itself. This leads to very similar results (consider that, roughly, 1 PgC/yr corresponds to 0.8 Sv). For this reason, only the main results will be summarized here, and the reader is left to Ludicone et al. (2008a) for details on the role of the different physical processes.

On the whole, the conversion of dense water into lighter water (the shallow overturning) is associated with the upward flux of ~ 10 PgC/yr of carbon, to which about ~ 12 PgC/yr are added by the transformation (cooling) of TW into SAMW. The dense water formation (the peak at about $\gamma=28.05$) is also ~ 10 PgC/yr. As discussed in Ludicone et al. (2008a), most of these diapycnal processes occur in relatively close proximity to the surface boundary layer of the ocean. The total diapycnal transport has been further decomposed into the components associated to the boundary buoyancy fluxes and to the mixing processes (Fig. 12). The buoyancy fluxes promote a larger DIC transport (the maximum is ~ 24 PgC/yr, from AAIW into SAMW) which is significantly compensated by mixing processes (which have a maximum transport of ~ 20 PgC/yr between the SAMW and the AAIW layers). Importantly, mixing promotes a significant flux of CDW into the surface layer in the AAIW class. This process, together with the lateral mixing in the mixed layer, sustains the outgassing observed in this density class, discussed in Sect. 4.

5.1.3 The DIC balance per water mass

To address how the redistribution of DIC by the thermohaline circulation compares with the total integrated effect of all sources and sinks of DIC, a quantitative balance of the

BGD

7, 3393–3451, 2010

Watermasses and the Southern Ocean carbon cycle

D. Ludicone et al.

Title Page

Abstract

Introduction

Conclusions

References

Tables

Figures

◀

▶

◀

▶

Back

Close

Full Screen / Esc

Printer-friendly Version

Interactive Discussion



sources and sinks per water mass can easily be evaluated using Eq. (9) (i.e., computing $\Delta\Psi_{\gamma}(\Theta)-\Delta\Phi_{\gamma}(\Theta)$ where the difference are between the values at the water mass boundaries). Under steady state conditions, this corresponds to integrating the sink/source terms over the water mass volume. We chose this latter approach in order to minimize the presence of errors in the calculation, since in the case of DIC these terms are orders of magnitude smaller than the transport terms and, thus, the computation of $\Delta\Psi_{\gamma}(\Theta)-\Delta\Phi_{\gamma}(\Theta)$ can reflect such errors if one is not careful. Also worthy of consideration is that the water mass volumes undergo large seasonal variations, e.g., large expanses of the surface layers south of the ACC fall in the AAIW class during the Austral Summer while in Winter they are in the CDW one (see Ludicone et al., 2008a and Ludicone et al., 2008c for a discussion). Therefore, the analysis, as well as in the case of $\Phi_{\gamma}(\Theta)$, is intrinsically Lagrangian since it refers to following the water mass volume over the year and not to the DIC balance over a specific oceanic region.

By integrating π_C (see Sect. 3 for details on the equation used in PISCES) over the isopycnal volumes, we have that on the whole the modeled Southern Ocean sink of DIC due to primary production (P) is 10.2 Pg C/yr. This value is very close to the value of the upwelling of DIC driven by the overturning. Remineralization (R) reconverts organic matter into DIC at a rate of 9.9 Pg C/yr, giving a net P-R balance of about -0.4 Pg C/yr (Fig. 14a) while the formation of CaCO_3 removes 0.2 Pg C/yr. Diffusive processes compensate the biological net loss by producing a net DIC increase of 0.6 Pg C/yr, while air-sea fluxes have an almost null budget (0.1 Pg C/yr). Since integrating the diffusive term over a closed volume corresponds to evaluating the diffusive fluxes at the boundary, the large-scale integrated effect of diffusion is dominated by the meridional flux at the northern boundary of the domain. The partitioning of these values into the different water masses, presented in Fig. 14a, reveals several interesting points. First, the deep remineralization drives the positive balance for deep water. The net effect of the difference between production and remineralization (P-R) is in fact the dominant term, which is the balance of terms that are on order of degrees larger than P-R itself. For the case of SAMW, the P-R net loss is compensated by diffusion and air-sea fluxes

BGD

7, 3393–3451, 2010

Watermasses and the Southern Ocean carbon cycle

D. Ludicone et al.

Title Page

Abstract

Introduction

Conclusions

References

Tables

Figures

◀

▶

◀

▶

Back

Close

Full Screen / Esc

Printer-friendly Version

Interactive Discussion



while the opposite is true for CDW. For the AAIW case, diffusive processes have to work against both the biological and air-sea flux terms. Partitioning the diffusive terms into their three components (not shown), the meridional flux is found to be mostly associated with CDW, while as expected, the DIC redistribution among the watermasses is largely due to vertical mixing. This sustains the transfer of DIC from deep layers to AAIW and SAMW. Finally, to ease the comparison with both the analysis of the air-sea CO_2 fluxes presented in Sect. 3, the same volume integral has been computed over the winter volume of the water mass (Fig. 14b). (Note that using a fixed volume over the year also simplifies the interpretation since as for the case $\int \partial C / \partial t d v = d / d t \int C d v$.) Since the seasonal variation of volume involves only the surface layers, keeping a fixed volume over the integration does not produce significant differences. The largest relative difference is a reduced role for TW processes (their winter volume is very small) and a higher P value for CDW, which is associated with production that actually occurs in summer when the surface waters are in the AAIW class. Finally, the same integral has been evaluated separately for the photic zone (here defined as the upper 120 m of the water column – Fig. 14c; and the deep layers – not shown). The photic zone presents a net loss of more than 1.0 Pg C/yr, and diffusion results in a flux in the opposite sense that largely compensates the biological production, while surface air-sea CO_2 fluxes play a secondary role. In fact only ~40% of the remineralization occurs at depth. See Fig. 14.

6 Lagrangian analysis of the 30° S volume and DIC transports

In Ludicone et al. (2008c), an extensive application of a quantitative Lagrangian approach was applied to the analysis of the physical component of the simulation (the ORCA2-LIM ice-ocean model output). The aim was to describe the global thermohaline circulation from a Southern Ocean perspective. More specifically, the study detailed the pathways of interbasin exchange via the Southern Ocean and the associated water mass transformations. Here the same approach is used to investigate the

BGD

7, 3393–3451, 2010

Watermasses and the Southern Ocean carbon cycle

D. Ludicone et al.

Title Page

Abstract

Introduction

Conclusions

References

Tables

Figures

◀

▶

◀

▶

Back

Close

Full Screen / Esc

Printer-friendly Version

Interactive Discussion



5 pathways of the DIC transport and redistribution in the Southern Ocean, where most of the global overturning occurs (Sloyan and Rintoul, 2001) and the associated DIC gain/loss driven by physical and biological processes. More specifically, as explained in the methods section, we used a Lagrangian approach to track the pathway of DIC into the watermasses. The results of the computation of volume pathways, of DIC transport pathways and of the corresponding losses/sinks are presented in Fig. 15.

10 The SAMW serves as the main exporter of DIC, as this watermass transports 59.4 Pg C/yr of DIC northward, with this transport largely exceeding the southward transport. SAMW originates in the SAZ in a region of deep mixed layers. Models and observations suggest that these layers are formed by a combination of cooling of subtropical gyre water and northward wind driven Ekman transport (Sarmiento et al., 2004). With our Lagrangian approach, we find that the origins of the non-recirculating SAMW are mostly TW (~70%) and the rest is coming from the shallow overturning of dense waters, as discussed in Ludicone et al. (2008a). In fact, the single net contribution from the overturning into SAMW results essentially from the downwelling of TW (16.3 Pg C/yr). In terms of gains/losses, waters that serve as a source of new SAMW loose DIC, since during the upwelling the CDW and AAIW loose DIC (-0.53 Pg C/yr), while the TW (the main source for the SAMW) gain DIC during the downwelling (0.38 Pg C/yr; mostly by air-sea fluxes and diffusive processes) but this gain is smaller than the loss of DIC.

20 The origin of the Intermediate Water that leaves the SO across 30° S is largely the recirculation and, partly, the downwelling of SAMW due to surface forcings and mixing and, as well, internal processes such as cabbeling. As with SAMW, the AAIW exports DIC but, rather surprisingly the export is very small relative to the export associated with SAMW. (The net volume export of AAIW from the Southern Ocean is actually small – see also Sloyan and Rintoul, 2001 – and this watermass has been somehow overlooked in the past, at least as compared to SAMW.) The overturning transport of DIC results mainly from the downwelling of the Mode Water, moreover this transformation causes a gain of DIC (0.09 Pg C/yr) greater than the loss of DIC due

BGD

7, 3393–3451, 2010

Watermasses and the Southern Ocean carbon cycle

D. Ludicone et al.

Title Page

Abstract

Introduction

Conclusions

References

Tables

Figures

◀

▶

◀

▶

Back

Close

Full Screen / Esc

Printer-friendly Version

Interactive Discussion



to the upwelling of denser waters. The CDW is the great importer of DIC toward the Southern Ocean. In fact, the Southern Ocean acts as a powerful converter of CDW (Ludicone et al., 2008a) since CDW are intensely transformed, partly feeding the AABW and partly feeding the AAIW, the SAMW and the TW. Interestingly, the CDW loses a great amount of DIC (-0.80 Pg C/yr) during the upwelling. The origin of the AABW that leaves the SO at 30° S is primarily the CDW. This water mass exports DIC toward north but the northward flux of the AABW gains DIC when it leaves the SO because the CDW, that downwells, gains DIC (via the process of remineralization).

7 Discussion

The main goal of this study was to characterize the large-scale processes controlling the DIC distribution in the Southern Ocean with a side discussion on its impact on DIC redistribution in the global ocean. This was approached analyzing the processes controlling the seasonal variations in air-sea CO_2 fluxes, i.e., sources and losses, and the processes at work in the ocean interior, i.e., transformation and redistribution. For the latter, we based our analysis on state-of-the-art approaches both in the Eulerian and Lagrangian frameworks, which were used for the first time, to the best of our knowledge, for analyzing reactive tracers dynamics in the ocean. In parallel we also exploited sensitive analysis tools to understand and weight the effects of biological production and remineralization vs. physico-chemical constraints on the large-scale distribution of DIC in the SO.

In such strongly seasonal oceanic region air-sea CO_2 fluxes should necessarily mirror seasonal variations. Our analysis showed that the leading terms driving those variations are sea surface DIC concentrations and temperature, with a relatively minor role, in terms of absolute upper layer CO_2 drawdown, played by biological production. As for the spatial dimension our analysis confirmed a functional “divide” in SO with a region of

BGD

7, 3393–3451, 2010

Watermasses and the Southern Ocean carbon cycle

D. Ludicone et al.

Title Page

Abstract

Introduction

Conclusions

References

Tables

Figures

◀

▶

◀

▶

Back

Close

Full Screen / Esc

Printer-friendly Version

Interactive Discussion



carbon uptake north of the SAF, and an outgassing region south of the SAF. The uptake region is also the region of formation of SAMW, with temperature being the dominant term controlling seasonal air-sea CO₂ fluxes, through winter cooling that increases, and summer heating that decreases, solubility. The outgassing region (with enhanced outgassing south of the PF) is where the intermediate and deeper waters upwell. In this region, south of the divide and differently from the northern region, seasonal variations in air-sea CO₂ fluxes are dominated by variations in DIC concentrations.

DIC concentrations in the surface layer, especially when they determine seasonal outgassing, result from the upwelling of DIC-rich deep water masses, driving an outgoing flux that is particularly strong in wintertime. ΔC_{gasex} analysis Mikaloff-Fletcher et al. (2007) suggests that carbon signature of SAMW is one of ingassing for both the Pacific and Atlantic basins and of outgassing for Antarctic Intermediate Water (AAIW), thus supporting the results of simulation. The implication is that exposure of internal DIC pool to the atmosphere forced by large scale circulation is a crucial term in CO₂ exchange between atmosphere and ocean. Still, having identified the SAF as dividing the Southern Ocean into an outgassing and an ingassing region, this consideration, coherent with previous analyses, puts a question on the limits of low resolution inversions. The main reasons for the mismatch between recent oceanic inversion and the known ocean dynamics are probably the scarcity of in situ data, the low resolution of the models used in support and the complexity of constraining the overturning in the region. Finally, for similar reasons, it is not surprising that the mismatch among the present day estimates of the anthropogenic carbon inventories is mainly in the Southern Ocean.

A striking feature of carbon cycle highlighted by our analysis is the very large difference (orders of magnitude) between the rates of DIC redistribution in the ocean interior due to large-scale oceanic processes and the net fluxes of CO₂ between the ocean and atmosphere at the sea surface. Indeed it is the latter that explicitly regulates the partitioning between the atmospheric and oceanic reservoirs, but it must be understood that those fluxes are largely pre-conditioned by internal oceanic mixing and transport

Watermasses and the Southern Ocean carbon cycle

D. Iudicone et al.

[Title Page](#)[Abstract](#)[Introduction](#)[Conclusions](#)[References](#)[Tables](#)[Figures](#)[⏪](#)[⏩](#)[◀](#)[▶](#)[Back](#)[Close](#)[Full Screen / Esc](#)[Printer-friendly Version](#)[Interactive Discussion](#)

processes. This in turn suggests that it is the internal distribution of DIC pool that is ultimately determining atmosphere-ocean fluxes.

Intriguingly, our model displays a positive bias in deep ocean DIC concentrations by as much as 2% in respect to the observed concentrations, which definitely is a significant amount if compared with the atmospheric pool. Paradoxically this stands as a very robust result, considering the orders-of-magnitude difference between the interior transformations/transport and the surface air-sea CO₂ fluxes. On the other hand this shows how finely tuned and complex must be the regulation of atmospheric concentration of CO₂, probably beyond our current understanding, to display the robust patterns registered over the climatic scale despite such overwhelming reservoir in the ocean interior. This result certainly motivate future work in this area but raises questions on our current representations of ocean carbon cycle.

Above we anticipated that biological processes do not seem to be dominating CO₂ fluxes on an annual base. We specifically analyzed the role of biological processes in controlling the 3-D distribution of DIC in the SO. The biological process influencing seasonal variations of DIC concentrations in the surface layer is primary production. This term is more important in areas where surface DIC concentration rules the exchange with atmosphere than in the areas where temperature control dominates. In other words, DIC removal by biota is more effective in areas where DIC concentration would produce outgassing, than in region where temperature would favour it. This is related to the fact that, light being available, regions of DIC concentration ruling CO₂ fluxes are rich in nutrients whereas regions of T ruling CO₂ fluxes are poor in nutrients. The role of light manifests in reducing surface DIC concentrations mostly in spring and summer, though with a minor influence on the air-sea CO₂ fluxes. This contrasts Takahashi et al. (2002) conclusions that biology plays an important role in transporting DIC from the surface to the deep ocean, thus suggesting that climate change perturbations to biology may be critical in perturbing carbon-climate feedbacks. Indeed, our results suggest that the role of biology is significantly smaller (by an order of magnitude) in regulating annual fluxes than transports associated with overturning.

Watermasses and the Southern Ocean carbon cycle

D. Iudicone et al.

Title Page

Abstract

Introduction

Conclusions

References

Tables

Figures



Back

Close

Full Screen / Esc

Printer-friendly Version

Interactive Discussion



Watermasses and the Southern Ocean carbon cycleD. Iudicone et al.

[Title Page](#)[Abstract](#)[Introduction](#)[Conclusions](#)[References](#)[Tables](#)[Figures](#)[◀](#)[▶](#)[◀](#)[▶](#)[Back](#)[Close](#)[Full Screen / Esc](#)[Printer-friendly Version](#)[Interactive Discussion](#)

We acknowledge that our model exhibits biases in carbon cycle reconstruction, possibly enhanced in the simulation of biological processes. Though, the large difference emerging by both Eulerian and Lagrangian diagnostics among the two classes of processes underscores the dominating importance of transport and transformation processes in the ocean interior, on the short term exchange between atmosphere and ocean. In particular, the role of the southward transport of sub-tropical waters in the formation of SAMW, a region of significant CO₂ ocean uptake, seems to be crucial for DIC redistribution and its implication for past and present carbon cycling have to be further explored. In addition, along with our inference about dependence of CO₂ drawdown on DIC concentration or temperature being also modulated by nutrients concentration, our approach shows a good potential to understand how the SAMW formation mechanism impact on nutrient redistribution in the ocean (e.g., Sarmiento et al., 2004, and Marinov et al., 2006).

The Southern Ocean has long been recognized as playing a central role in the response of the global carbon cycle and biological productivity to the climate change (e.g., Sarmiento et al., 2004). The similarities between changes in atmospheric CO₂ and Antarctic temperature suggest that the Southern Ocean plays a critical role in regulating the glacial-interglacial CO₂ changes (Petit et al., 1999). The transition from the Last Glacial Maximum (LGM) to the Holocene was characterized by an increased atmospheric CO₂ concentration of ~40% (Monnin et al., 2001). This rise in atmospheric CO₂ closely followed the rise in East Antarctic temperatures, implying that the ocean's release of carbon to the atmosphere was associated with changes in the Southern Ocean (Marchitto et al., 2007).

While our analysis was not aimed to address those issues we can say that all the physical processes considered so far may be candidate to modulate partitioning of CO₂ between atmosphere and ocean on a short time scale. They include perturbations to the density stratification of Southern Ocean surface waters, the extent of sea ice coverage (Marchitto et al., 2007), or changes in the northward wind-driven Ekman transport (Sarmiento et al., 2004). Collectively or separately these processes may

contribute to slightly change the exposure time of deep waters to the atmosphere or to change the mixture ratio of CDW and TW in the SAMW formation thus changing CO₂ annual fluxes.

For example it has been argued that, during last deglaciation, deep convection was restored after a time interval of weak or absent activity as a consequence of ice cover retreat (Gersonde et al., 2005). This would have redistributed carbon transporting it from the abyss to upper ocean and atmosphere. In fact, since this last transition the concentration of atmospheric CO₂ grew to a value of ~280 ppmv. What we can qualitatively infer from our dynamical reconstruction is that restoring deep convection would have imposed a significant time lag before exposing DIC rich waters to the atmosphere. Parallel mechanisms may have occurred producing a similar effect on a short time scale, such as progressive warming in the region of SAMW formation, decrease in production south of the SAF, etc. This explains the uncertainty in predicting the response of the carbon cycle in the Southern Ocean to climate change as testified by the projections of the climate-carbon feedbacks (Sarmiento et al., 1998; Friedlingstein et al., 2003, 2006, and Roy et al., 2010).

Our simulation applies to the long term climatic scale without considering recent anthropogenic perturbation. Sarmiento et al. (1998) argued that 21st century climate change could result in changes in the physical state of the ocean such that ocean uptake of anthropogenic carbon could be reduced in the future. They also argued that the causing process, i.e., increased stratification could produce a positive feedback on the climate system. Parallel modeling work by Le Quéré et al. (2007) with a full representation of the natural carbon cycle emphasized that both anthropogenic carbon and natural carbon cycle would be perturbed also by other process. Secular trends toward increased wind strength over the Southern Ocean would increase outgassing of CO₂, which would compensate for the increased potential for ingassing due to the anthropogenic increase in DIC atmospheric concentration. Our study sets a baseline for comparing pre-anthropogenic and recent DIC redistribution in the ocean. More important our study provide a 3-D reconstruction of the processes ruling CO₂ exchanges

BGD

7, 3393–3451, 2010

Watermasses and the Southern Ocean carbon cycle

D. Iudicone et al.

Title Page

Abstract

Introduction

Conclusions

References

Tables

Figures

◀

▶

◀

▶

Back

Close

Full Screen / Esc

Printer-friendly Version

Interactive Discussion



while previous analyses were focused on Ekman upwelling intensity and frontal positions, i.e., surface processes, not sufficient to constrain the dynamics.

Marinov et al. (2006) previously argued that the Polar Front provides a “Biogeochemical Divide” that separates the Southern Ocean into two important regions, which are distinguished by their controls on air-sea CO₂ fluxes and biological production. Here we have shown that these surface delimited regions are tightly connected with large-scale overturning and water mass transformation processes. This has two implications. First, the 3-D dynamics is the driver of the surface gradient which determine fluxes at a given time and, secondly, the 3-D integrated methods described here to analyze ocean circulation and tracer distributions can also be exploited to characterize variability on several time scales from the interannual to the millennial.

8 Conclusions

We have analyzed the Southern Ocean carbon cycle through a pre-industrial simulation of a biogeochemical model coupled with an ocean circulation model. The air-sea CO₂ flux computed with our model shows that south of the PF the Southern Ocean is a strong source of CO₂ in agreement with an upwelled DIC from the AAIW and CDW. North of the SAF the Southern Ocean is a sink of CO₂ in agreement with an increased effect of the temperature on the air-sea CO₂ flux. Thanks to our sensitivity analysis we have revealed that the temperature and DIC are the most important variables regulating the air-sea CO₂ flux. Moreover concerning the biological processes that can influence the surface DIC concentration and as a consequence the air-sea CO₂ flux, the production term of the equation of DIC (i.e. the export of carbon through the primary production) is the most important variable regulating the DIC concentrations in summer and spring, but in the region of outgassing its effect is inefficient because well contrasted from the temperature effect. On the other hand the vertical diffusivity is the main physical variables regulating the DIC concentration that instead influences also the air-sea CO₂ flux causing an intense positive flux in winter. Regarding the

Watermasses and the Southern Ocean carbon cycle

D. Iudicone et al.

Title Page

Abstract

Introduction

Conclusions

References

Tables

Figures

◀

▶

◀

▶

Back

Close

Full Screen / Esc

Printer-friendly Version

Interactive Discussion



lagrangian analysis, we have computed the pathway of the main water masses, the respective transport and the associated DIC gain and loss of the water masses leaving the Southern Ocean at 30° S. We have shown that the upwelling of denser water that flow northward loose DIC, while the downwelling of lighter water gain DIC when they leaves the Southern Ocean at 30° S. From our study results that the SAMW have a great relevance both in the surface layer at the air-sea interface and in the overturning into the water column. The SAMW is the main water mass that export DIC from the Southern Ocean, moreover the overturning of denser waters in SAMW that flow northward causes a loss of DIC greater that the gain due to the overturning of the TW although it represents the main source for the SAMW. The AAIW also export DIC but it is not much, moreover it gains DIC due to the downwelling of denser waters (principally SAMW) that leaves the Southern Ocean as AAIW. Finally the CDW are intensely transformed and loose a great amount of DIC during their transformation in lighter waters and their flow northward. Our future perspective will be to repeat the analysis with an anthropogenic simulation with the aims of a better understanding of the future Southern Ocean role in the global carbon cycle. The implications on the global nutrient dynamics of the processes and sources involved in the mode water formation will also be assessed with a specific analysis.

Appendix A

Model description

The biogeochemical model PISCES is based on HAMOCC5 (Aumont et al., 2003) and simulates the biogeochemical cycle of oxygen, carbon and of the main nutrients that control marine phytoplankton growth: nitrate and ammonium, phosphate, silicate and iron (Aumont et al., 2003, Aumont and Bopp, 2006). The Redfield ratio is constant and phytoplankton growth is limited by the external availability of nutrients. The cycle of carbon and nitrogen are decoupled in the model to a certain degree by nitrogen fixation

Watermasses and the Southern Ocean carbon cycle

D. Iudicone et al.

Title Page

Abstract

Introduction

Conclusions

References

Tables

Figures



Back

Close

Full Screen / Esc

Printer-friendly Version

Interactive Discussion



and denitrification (Gehlen et al., 2006). PISCES has twenty-four compartments. There are five limiting nutrients for phytoplankton growth (nitrate, ammonium, phosphate, silicate and iron). Four living compartments: two phytoplankton size-classes corresponding to nanophytoplankton and diatoms and two zooplankton size classes which are microzooplankton and mesozooplankton. The phytoplankton is represented in total biomass, iron, chlorophyll and silicon contents. The zooplankton is modeled only in total biomass. There are three non-living compartments: semi-labile dissolved organic matter, small and big sinking particles. The iron, silicon and calcite pools of particles are explicitly modeled. In addition to the ecosystem model, PISCES also simulates dissolved inorganic carbon, total alkalinity and dissolved oxygen.

In the ice-ocean coupled model ORCA2-LIM, LIM is the sea ice model (Fichefet and Maqueda, 1997, Timmermann et al., 2005). It is a fully dynamical-thermodynamical sea ice model. The ocean model is the OPA model (Madec et al., 1998, Delecluse and Madec, 1999) in its global configuration ORCA2. The horizontal mesh is based on a 2° by 2° Mercator grid. There are 31 levels in the vertical, with the highest resolution (10 m) in the upper 150 m. The upper boundary uses a free surface formulation (Roullet and Madec, 2000). Lateral mixing is evaluated along isoneutral surfaces. The model is supplemented with the Gent and McWilliams (1990) parameterization. The lateral mixing coefficient depends on the baroclinic instability growth rate (Treguier et al., 1997). The vertical mixing scheme uses a turbulent closure (Blanke and Delecluse, 1993), and there is a diffusive bottom boundary layer parameterization (Beckmann and Doscher, 1997). The model background vertical diffusivity increases from the surface to the bottom in order to mimic the effects of decreased stratification and increased small-scale turbulence near the bottom (Values ranges from $0.12 \cdot 10^{-4} \text{ m}^2 \text{ s}^{-1}$ in the first 1000 m to $1.2 \cdot 10^{-4} \text{ m}^2 \text{ s}^{-1}$ at depth). Convection is emulated via an enhanced vertical diffusivity. At surface the ocean model is forced by computing fluxes of heat and freshwater (evaporation) by means of bulk formulae and using monthly climatologies of atmospheric forcings. A penetrative shortwave solar radiation formulation is used. A restoring to climatological surface salinities was also added. Climatological ERS1/2 scatterometer

Watermasses and the Southern Ocean carbon cycle

D. Iudicone et al.

Title Page

Abstract

Introduction

Conclusions

References

Tables

Figures

◀

▶

◀

▶

Back

Close

Full Screen / Esc

Printer-friendly Version

Interactive Discussion



monthly mean wind stresses were used for the tropics while the NCEP/NCAR climatology was used poleward of 50° N and 50° S. In low and intermediate resolution OGCM, time variability is in most case limited to forcing variability and thus for the analysis we used a model time sampling of 14.6 days to resolve the main time scale of the forcing.

Consistently, we used a same model time sampling in the biogeochemical model.

Acknowledgements. We gratefully acknowledge the support by Vincenzo Saggiomo. The data of the natural carbon oceanic inversion were kindly provided by Nicolas Gruber. We would like to thank Sarah E. Mikaloff Fletcher for helpful discussions and suggestions. Discussion with B. Linne' are also kindly acknowledged. The work was partly done in the framework of PEA-CANOPO and VECTOR Projects.

This work is dedicated to the memory of Volfango Rupolo, a mentor in both oceanography and life for DI, and above all a dear friend for 20 years. Volfango died 5 April 2010, at the age of 46 years and one day.

References

- Anderson, R. F., Ali, S., Bradtmiller, L. I., Nielsen, S. H. H., Fleisher, M. Q., Anderson, B. E., and Burckle, L. H.: Wind-driven upwelling in the Southern Ocean and the deglacial rise in atmospheric CO₂, *Science*, 323, 1443–1448, 2009. 3396, 3397, 3437
- Aumont, O. and Bopp, L.: Globalizing results from ocean in situ iron fertilization studies, *Global Biogeochem. Cy.*, 20, GB2017, doi:10.1029/2005GB002591, 2006. 3426
- Aumont, O., Maier-Reimer, E., Blain, S., and Monfray, P.: An ecosystem model of the global ocean including Fe, Si, P colimitations, *Global Biogeochem. Cy.*, 17, 1060, doi:10.1029/2001GB001745, 2003. 3426
- Beckmann, A. and Doscher, R.: A method for improved representation of dense water spreading over topography in geopotential-coordinate models, *J. Phys. Oceanogr.*, 27, 581–591, 1997. 3427
- Belkin, I. M. and Gordon, A. L.: Southern Ocean fronts from the Greenwich meridian to Tasmania, *J. Geophys. Res.*, 101, 3675–3696, 1996. 3440
- Bindoff, N. L. and McDougall, T. J.: Diagnosing climate change and ocean ventilation using hydrographic data, *J. Phys. Oceanogr.*, 24, 1137–1152, 1994. 3396

Watermasses and the Southern Ocean carbon cycle

D. Iudicone et al.

Title Page

Abstract

Introduction

Conclusions

References

Tables

Figures

⏪

⏩

◀

▶

Back

Close

Full Screen / Esc

Printer-friendly Version

Interactive Discussion



Watermasses and the Southern Ocean carbon cycle

D. Iudicone et al.

[Title Page](#)
[Abstract](#)
[Introduction](#)
[Conclusions](#)
[References](#)
[Tables](#)
[Figures](#)
[Back](#)
[Close](#)
[Full Screen / Esc](#)
[Printer-friendly Version](#)
[Interactive Discussion](#)


Blanke, B. and Delecluse, P.: Variability of the tropical Atlantic-ocean simulated by a general-circulation model with 2 different mixed-layer physics, *J. Phys. Oceanogr.*, 23, 1363–1388, 1993. 3427

Blanke, B. and Raynaud, S.: Kinematics of the Pacific equatorial undercurrent: An Eulerian and Lagrangian approach from GCM results, *J. Phys. Oceanogr.*, 27, 1038–1053, 1997. 3403

Delecluse, P. and Madec, G.: Ocean modelling and the role of the ocean in the climate system, in: *Modeling the Earth's climate and its variability*, edited by: Holland, W. R., Jousaume, S., and David, F., vol. 67 of *Les Houches summer school session*, 237–313 pp., 1999. 3427

Dutay, J., Emile-Geay, J., Iudicone, D., Jean-Baptiste, P., Madec, G., and Carouge, C.: Helium isotopic constraints on simulated ocean circulations: implications for abyssal theories, *Environ. Fluid Mech.*, 10, 257–273, doi:10.1007/s10652-009-9159-y, 2009. 3404

Feely, R. A., Sabine, C. L., Takahashi, T., and Wanninkhof, R.: Uptake and storage of carbon dioxide in the ocean, *Oceanography*, 14, 18–32, 2001. 3401

Fichefet, T. and Maqueda, M. A. M.: Sensitivity of a global sea ice model to the treatment of ice thermodynamics and dynamics, *J. Geophys. Res.*, 102, 12609–12646, 1997. 3427

Friedlingstein, P., Dufresne, J. L., Cox, P. M., and Rayner, P.: How positive is the feedback between climate change and the carbon cycle?, *Tellus B*, 55, 692–700, 2003. 3424

Friedlingstein, P., Cox, P., Betts, R., Bopp, L., Von Bloh, W., Brovkin, V., Cadule, P., Doney, S., Eby, M., Fung, I., Bala, G., John, J., Jones, C., Joos, F., Kato, T., Kawamiya, M., Knorr, W., Lindsay, K., Matthews, H. D., Raddatz, T., Rayner, P., Reick, C., Roeckner, E., Schnitzler, K. G., Schnur, R., Strassmann, K., Weaver, A. J., Yoshikawa, C., and Zeng, N.: Climate-carbon cycle feedback analysis: Results from the (CMIP)-M-4 model intercomparison, *J. Climate*, 19, 3337–3353, 2006. 3424

Gehlen, M., Bopp, L., Emprin, N., Aumont, O., Heinze, C., and Ragueneau, O.: Reconciling surface ocean productivity, export fluxes and sediment composition in a global biogeochemical ocean model, *Biogeosciences*, 3, 521–537, 2006, <http://www.biogeosciences.net/3/521/2006/>. 3427

Gent, P. R. and McWilliams, J. C.: Isopycnal mixing in ocean circulation models, *J. Phys. Oceanogr.*, 20, 150–155, 1990. 3427

Gersonde, R., Crosta, X., Abelmann, A., and Armand, L.: Sea-surface temperature and sea ice distribution of the Southern Ocean at the EPILOG Last Glacial Maximum A circum-Antarctic view based on siliceous microfossil records, *Quaternary Sci. Rev.*, 24, 869–896, 2005. 3424

Watermasses and the Southern Ocean carbon cycle

D. Iudicone et al.

Title Page

Abstract

Introduction

Conclusions

References

Tables

Figures

◀

▶

◀

▶

Back

Close

Full Screen / Esc

Printer-friendly Version

Interactive Discussion



Gloor, M. N., Sarmiento, J. L., Sabine, C. L., Feely, R. A., and Rödenbeck, C.: A first estimate of present and preindustrial air-sea CO₂ flux patterns based on ocean interior carbon measurements and models, *Geophys. Res. Lett.*, 30, 1010, doi:10.1029/2002GL015594, 2003. 3410

5 Greatbatch, R. J. and Zhai, X.: The Generalized heat function, *Geophys. Res. Lett.*, 34, L21601, doi:10.1029/2007GL031427, 2007. 3415

Gruber, N., Sarmiento, J. L., and Stocker, T. F.: An improved method for detecting anthropogenic CO₂ in the oceans, *Global Biogeochem. Cy.*, 10, 809–837, 1996. 3398

10 Gruber, N., Gloor, M., Fletcher, S., Doney, S., Dutkiewicz, S., Follows, M., Gerber, M., Jacobson, A., Joos, F., Lindsay, K., et al.: Oceanic sources, sinks, and transport of atmospheric CO₂, *Global Biogeochem. Cy.*, 23, GB1005, doi:10.1029/2008GB003349, 2009. 3405

Ito, T., Parekh, P., Dutkiewicz, S., and Follows, M. J.: The Antarctic Circumpolar Productivity Belt, *Geophys. Res. Lett.*, 32, L13604, doi:10.1029/2005GL023021, 2005. 3406

15 Iudicone, D., Madec, G., Blanke, B., and Speich, S.: The role of Southern Ocean surface forcings and mixing in the global conveyor, *J. Phys. Oceanogr.*, 38, 1377–1400, 2008a. 3397, 3398, 3399, 3403, 3404, 3416, 3417, 3419, 3420, 3434, 3448

Iudicone, D., Madec, G., and McDougall, T. J.: Water-mass transformations in a neutral density framework and the key role of light penetration, *J. Phys. Oceanogr.*, 38, 1357–1376, 2008b. 3401, 3414, 3415

20 Iudicone, D., Speich, S., Madec, G., and Blanke, B.: The global conveyor belt from a Southern Ocean perspective, *J. Phys. Oceanogr.*, 38, 1401–1425, 2008c. 3398, 3399, 3403, 3404, 3405, 3417, 3418, 3437

Jackett, D. R. and McDougall, T. J.: A neutral density variable for the worlds oceans, *J. Phys. Oceanogr.*, 27, 237–263, 1997. 3401

25 Key, R. M., Kozyr, A., Sabine, C., Lee, K., Wanninkhof, R., Bullister, J., Feely, R., Millero, F., Mordy, C., and Peng, T.: A global ocean carbon climatology: Results from Global Data Analysis Project (GLODAP), *Global Biogeochem. Cy.*, 18, GB4031, doi:10.1029/2004GB002247, 2004. 3397, 3405

30 Le Quéré, C., Rodenbeck, C., Buitenhuis, E., Conway, T., Langenfelds, R., Gomez, A., Labuschagne, C., Ramonet, M., Nakazawa, T., Metzl, N., et al.: Saturation of the Southern Ocean CO₂ sink due to recent climate change, *Science*, 316, 1735–1738, 2007. 3424

Lumpkin, R. and Speer, K.: Global ocean meridional overturning, *J. Phys. Oceanogr.*, 37, 2550–2562, 2007. 3396

- Naveira Garabato, A. C., Stevens, D. P., Watson, A. J., and Roether, W.: Short-circuiting of the oceanic overturning circulation in the Antarctic Circumpolar Current, *Nature*, 447, 194–197, 2007. 3397, 3437
- Petit, J. R., Jouzel, J., Raynaud, D., Barkov, N., Barnola, J., Basile, I., Bender, M., Chappellaz, J., Davis, M., Delaygue, G., et al.: Climate and atmospheric history of the past 420 000 years from the Vostok ice core, *Antarctica, Nature*, 399, 429–436, 1999. 3423
- Pollard, R. T., Lucas, M. I., and Read, J. F.: Physical controls on biogeochemical zonation in the Southern Ocean, *Deep-Sea Res. Pt. II*, 49, 3289–3305, 2002. 3406
- Radenac, M. H., Dandonneau, Y., and Blanke, B.: Displacements and transformations of nitrate-rich and nitrate-poor water masses in the tropical Pacific during the 1997 El Niño, *Ocean Dynam.*, 55, 34–46, 2005. 3403
- Roulet, G. and Madec, G.: Salt conservation, free surface, and varying levels: a new formulation for ocean general circulation models, *J. Geophys. Res.*, 105, 23927–23942, 2000. 3427
- Sabine, C. L., Feely, R., Gruber, N., Key, R., Lee, K., Bullister, J., Wanninkhof, R., Wong, C., Wallace, D., Tilbrook, B., et al.: The oceanic sink for anthropogenic CO₂, *Science*, 305, 367, 2004. 3399
- Sarmiento, J. L., Gruber, N., Brzezinski, M. A., and Dunne, J. P.: High-latitude controls of thermocline nutrients and low latitude biological productivity, *Nature*, 427, 56–60, 2004. 3396, 3397, 3419, 3423
- Sarmiento, J. L., Hughes, T. M. C., Stouffer, R. J., and Manabe, S.: Simulated response of the ocean carbon cycle to anthropogenic climate warming, *Nature*, 393, 245–249, 1998. 3424
- Sloyan, B. M. and Rintoul, S. R.: The Southern Ocean limb of the global deep overturning circulation, *J. Phys. Oceanogr.*, 31, 143–173, 2001. 3406, 3419
- Speer, K., Rintoul, S. R., and Sloyan, B.: The diabatic Deacon cell, *J. Phys. Oceanogr.*, 30, 3212–3222, 2000. 3396
- Sverdrup, H. U., Johnson, M. W., and Fleming, R. H.: *The oceans, their physics, chemistry, and general biology*, Prentice-Hall, inc., 1942. 3406
- Takahashi, T., Olafsson, J., Goddard, J. G., Chipman, D. W., and Sutherland, S. C.: Seasonal variation of CO₂ and nutrients in the high-latitude surface oceans: a comparative study, *Global Biogeochem. Cy.*, 7, 843–878, 1993. 3409, 3410

BGD

7, 3393–3451, 2010

Watermasses and the Southern Ocean carbon cycleD. Iudicone et al.

Title Page

Abstract

Introduction

Conclusions

References

Tables

Figures

◀

▶

◀

▶

Back

Close

Full Screen / Esc

Printer-friendly Version

Interactive Discussion



Watermasses and the Southern Ocean carbon cycle

D. Iudicone et al.

[Title Page](#)
[Abstract](#)
[Introduction](#)
[Conclusions](#)
[References](#)
[Tables](#)
[Figures](#)
[◀](#)
[▶](#)
[◀](#)
[▶](#)
[Back](#)
[Close](#)
[Full Screen / Esc](#)
[Printer-friendly Version](#)
[Interactive Discussion](#)


- Takahashi, T., Sutherland, S., Sweeney, C., Poisson, A., Metzl, N., Tilbrook, B., Bates, N., Wanninkhof, R., Feely, R., Sabine, C., et al.: Global sea-air CO₂ flux based on climatological surface ocean pCO₂, and seasonal biological and temperature effects, *Deep-Sea Res. Pt. II*, 49, 1601–1622, 2002. 3401, 3409, 3422
- 5 Takahashi, T., Sutherland, S., Wanninkhof, R., Sweeney, C., Feely, R., Chipman, D., Hales, B., Friederich, G., Chavez, F., Sabine, C., et al.: Climatological mean and decadal change in surface ocean pCO₂, and net sea-air CO₂ flux over the global oceans, *Deep-Sea Res. Pt. II*, 56, 554–577, 2009. 3398, 3401, 3405
- Talley, L. D., Reid, J. L., and Robbins, P. E.: Data-based meridional overturning streamfunctions for the global ocean, *J. Climate*, 16, 3213–3226, 2003. 3397, 3437
- 10 Timmermann, R., Goosse, H., Madec, G., Fichefet, T., Ette, C., and Dulière, V.: On the representation of high latitude processes in the ORCA-LIM global coupled sea ice-ocean model, *Ocean Model.*, 8, 175–201, doi:10.1016/j.ocemod.2003.12.009, 2005. 3427
- Treguier, A. M., Held, I. M., and Larichev, V. D.: Parameterization of quasigeostrophic eddies in primitive equation ocean models, *J. Phys. Oceanogr.*, 27, 567–580, 1997. 3427
- 15 Walin, G.: On the relation between sea-surface heat flow and thermal circulation in the ocean, *Tellus*, 34, 187, 1982. 3414
- Wanninkhof, R.: Relationship between wind speed and gas exchange, *J. Geophys. Res.*, 97, 7373–7382, 1992. 3400
- 20 Weiss, R. F.: Carbon dioxide in water and seawater: the solubility of a non-ideal gas, *Mar. Chem.*, 2, 203–215, 1974. 3400
- Zika, J. D., Sloyan, B. M., and McDougall, T. J.: Diagnosing the Southern Ocean Overturning from Tracer Fields, *J. Phys. Oceanogr.*, 39, 2926–2940, 2009. 3397

Watermasses and the Southern Ocean carbon cycle

D. Iudicone et al.

Table 1. Definition of water masses used in the text. Acronyms are: Thermocline Water (TW), Mode Water (SAMW), Intermediate Water (AAIW), Upper Circumpolar Water (UCDW), Lower Circumpolar Water (LCDW) and Antarctic Bottom Water (AABW). The neutral density values of the boundaries between water masses have been defined on the base of a detailed analysis of the model physical fields (Iudicone et al., 2008a). Notice, in particular, that the model AAIW is cooler and thus denser than climatological in situ values.

Water masses	γ
TW	0–26.0
SAMW	26.0–27.2
AAIW	27.2–27.8
UCDW	27.8–28.0
LCDW	28.0–28.2
AABW	28.2–Bottom

Title Page

Abstract

Introduction

Conclusions

References

Tables

Figures

◀

▶

◀

▶

Back

Close

Full Screen / Esc

Printer-friendly Version

Interactive Discussion



Table 2. Seasonal mean of air-sea CO₂ flux in mol/m²/yr computed in offline (Offline flux), without the effect of temperature (Flux-T), without the effect of DIC (flux-DIC), the distance between the offline flux and the flux without the effect of DIC (DIC Signal), the distance between the offline flux and the flux without the effect of T (T Signal), and the difference between the DIC signal and the T signal (DIC-T), the positive values mean that the DIC signal prevail the T signal while negative values mean that the T signal prevail the DIC signal.

		Water masses						
Winter	Offline Flux	-1.94	-1.91	0.91	1.81	1.38	2.03	
	Flux-DIC	-2.22	-2.82	-1.25	0.41	0.55	1.05	
	Flux-T	-0.56	-0.03	2.71	2.16	1.41	2.01	
	DIC signal	0.28	0.92	2.16	1.41	0.82	0.98	
	T signal	1.38	1.87	1.8	0.35	0.03	0.01	
	DIC-T	-1.10	-0.96	0.36	1.06	0.8	0.96	
Spring	Offline Flux	-0.80	-0.86	0.94	1.81	1.41	1.42	
	Flux-DIC	-0.92	-1.29	0.14	1.95	1.7	1.32	
	Flux-T	-0.54	-0.41	1.39	1.98	1.46	1.44	
	DIC signal	0.12	0.43	0.8	0.14	0.29	0.1	
	T signal	0.26	0.44	0.45	0.17	0.06	0.02	
	DIC-T	-0.15	-0.01	0.35	-0.03	0.23	0.08	
Summer	Offline Flux	0.31	0.29	1.31	2.01	1.74	0.46	
	Flux-DIC	0.52	0.98	3.7	6.58	6.11	2.42	
	Flux-T	-0.87	-1.43	-1.02	0.49	1.33	0.4	
	DIC signal	0.21	0.69	2.39	4.57	4.37	1.96	
	T signal	1.17	1.72	2.33	1.52	0.41	0.06	
	DIC-T	-0.96	-1.03	0.07	3.06	3.96	1.9	
Fall	Offline Flux	-0.79	-1.47	-0.45	1.15	0.82	1.56	
	Flux-DIC	-0.55	-0.73	0.99	2.09	0.98	1.29	
	Flux-T	-1.08	-1.79	-0.42	1.26	0.87	1.57	
	DIC signal	0.24	0.75	1.44	0.95	0.15	0.27	
	T signal	0.29	0.32	0.03	0.11	0.05	0.01	
	DIC-T	-0.04	0.43	1.4	0.83	0.11	0.27	
Annual	Offline Flux	-0.85	-1.02	0.69	1.7	1.34	1.39	
	Flux-DIC	-0.85	-1.04	0.81	2.66	2.26	1.5	
	Flux-T	-0.75	-0.88	0.75	1.5	1.27	1.38	
	DIC signal	0.00	0.01	0.12	0.97	0.92	0.11	
	T signal	0.10	0.14	0.06	0.2	0.07	0.01	
	DIC-T	-0.10	-0.13	0.06	0.77	0.86	0.1	

Table 3. Seasonal mean of air-sea CO₂ flux in PgC/yr computed offline (Offline flux), without the effect of temperature (Flux-T), without the effect of DIC (flux-DIC), the distance between the offline flux and the flux without the effect of DIC (DIC Signal), the distance between the offline flux and the flux without the effect of T (T Signal), and the difference between the DIC signal and the T signal (DIC-T), the positive values mean that the DIC signal prevails over the T signal while negative values mean that the T signal prevails over the DIC signal.

		Water masses					
		TW	SAMW	AAIW	UCDW	LCDW	AABW
Winter	Offline Flux	-0.18	-1.06	0.38	0.25	0.05	0.02
	Flux-DIC	-0.20	-1.57	-0.52	0.06	0.02	0.01
	Flux-T	-0.05	-0.02	1.13	0.30	0.05	0.02
	DIC signal	0.03	0.51	0.90	0.19	0.03	0.01
	T signal	0.13	1.04	0.75	0.05	0.00	0.00
	DIC-T	-0.10	-0.53	0.15	0.15	0.03	0.01
Spring	Offline Flux	-0.07	-0.48	0.39	0.25	0.05	0.01
	Flux-DIC	-0.08	-0.71	0.06	0.27	0.06	0.01
	Flux-T	-0.05	-0.23	0.58	0.27	0.05	0.01
	DIC signal	0.01	0.24	0.33	0.02	0.01	0.00
	T signal	0.02	0.25	0.19	0.02	0.00	0.00
	DIC-T	-0.01	-0.01	0.15	0.00	0.01	0.00
Summer	Offline Flux	0.03	0.16	0.55	0.28	0.06	0.00
	Flux-DIC	0.05	0.55	1.54	0.91	0.22	0.02
	Flux-T	-0.08	-0.79	-0.42	0.07	0.05	0.00
	DIC signal	0.02	0.38	1.00	0.63	0.16	0.02
	T signal	0.11	0.96	0.97	0.21	0.01	0.00
	DIC-T	-0.09	-0.57	0.03	0.42	0.14	0.02
Fall	Offline Flux	-0.07	-0.82	-0.19	0.16	0.03	0.02
	Flux-DIC	-0.05	-0.40	0.41	0.29	0.03	0.01
	Flux-T	-0.10	-0.99	-0.17	0.17	0.03	0.02
	DIC signal	0.02	0.41	0.60	0.13	0.01	0.00
	T signal	0.03	0.18	0.01	0.02	0.00	0.00
	DIC-T	0.00	0.24	0.59	0.12	0.00	0.00
Annual	Offline Flux	-0.08	-0.57	0.29	0.23	0.05	0.01
	Flux-DIC	-0.08	-0.58	0.34	0.37	0.08	0.02
	Flux-T	-0.07	-0.49	0.31	0.21	0.05	0.01
	DIC signal	0.00	0.01	0.05	0.13	0.03	0.00
	T signal	0.01	0.08	0.03	0.03	0.00	0.00
	DIC-T	-0.01	-0.07	0.03	0.11	0.03	0.00

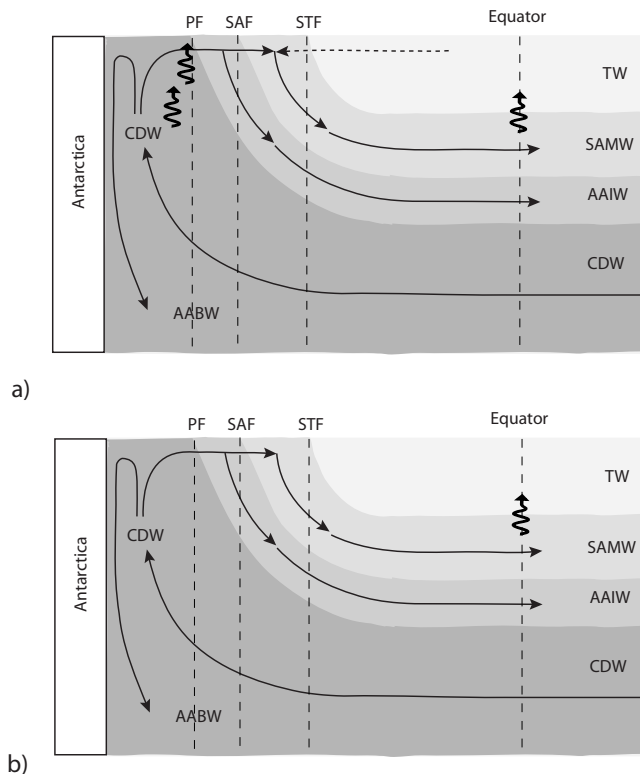


Fig. 1. Schematics of the overturning circulation in the Southern Ocean. Panel **(a)** accounts for both a major TW contribution to SAMW formation (e.g., Talley et al., 2003; Iudicone et al., 2008c) as well as a significant role for diapycnal transports below the base of the mixed layer in the upwelling of CDW over the Southern Ocean (e.g., Naveira Garabato et al., 2007; Iudicone et al., 2008c). Panel **(b)** assumes that CDW is the primary source for both AAIW and SAMW, and that transformations between these water masses are dominated by processes occurring in the mixed layer (e.g., Anderson et al., 2009).

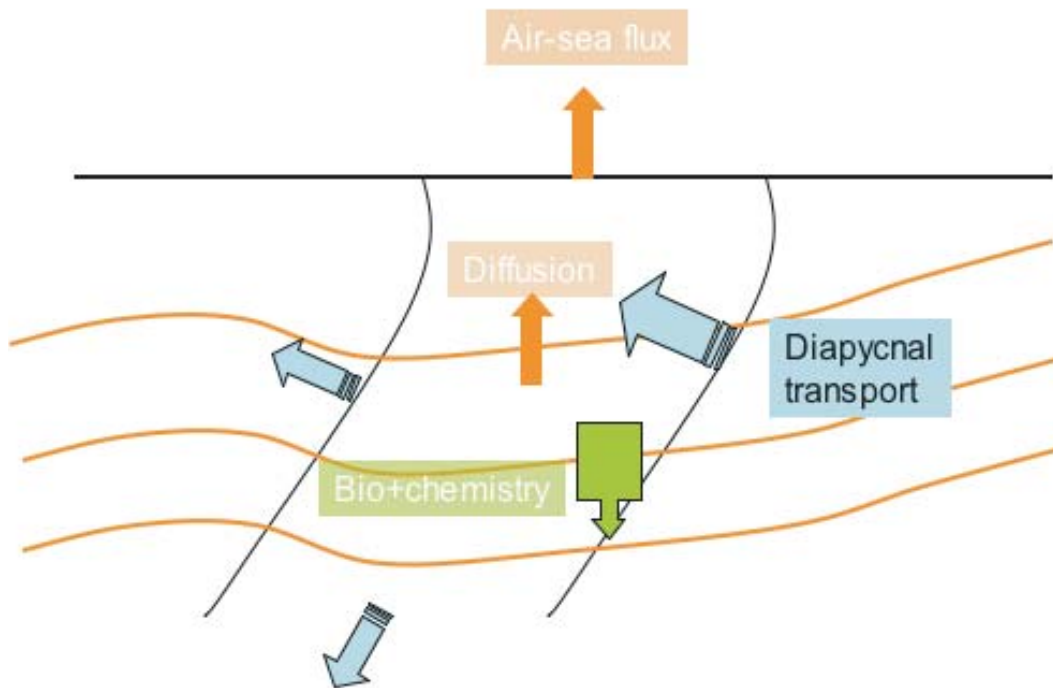


Fig. 2. Sketch of the tracer C balance in an isopycnal framework.

Watermasses and the Southern Ocean carbon cycle

D. Iudicone et al.

Title Page	
Abstract	Introduction
Conclusions	References
Tables	Figures
◀	▶
◀	▶
Back	Close
Full Screen / Esc	
Printer-friendly Version	
Interactive Discussion	



Watermasses and the Southern Ocean carbon cycle

D. Iudicone et al.

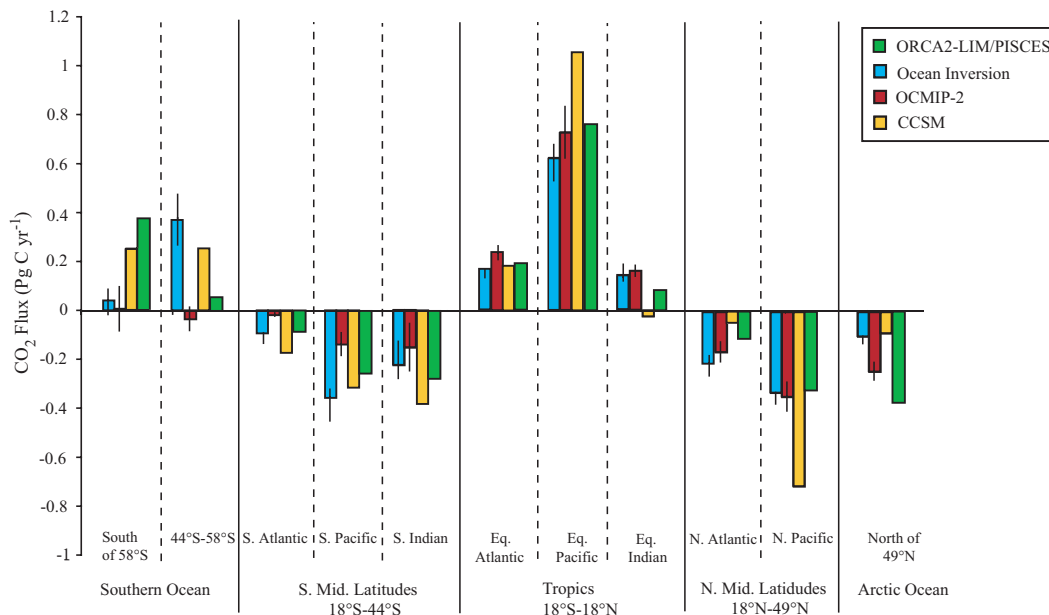


Fig. 3. Comparison between the air-sea CO₂ flux from PISCES and from the results published by Mikaloff-Fletcher et al. (2007): ocean inversion, forward simulation from OCMIP-2, and forward simulation from the CCSM coupled with the ecosystem and biogeochemical model described by Moore et al. (2004). [Modified from Mikaloff-Fletcher et al., 2007]

Discussion Paper | Discussion Paper | Discussion Paper | Discussion Paper | Discussion Paper

Title Page

Abstract Introduction

Conclusions References

Tables Figures

◀ ▶

◀ ▶

Back Close

Full Screen / Esc

Printer-friendly Version

Interactive Discussion



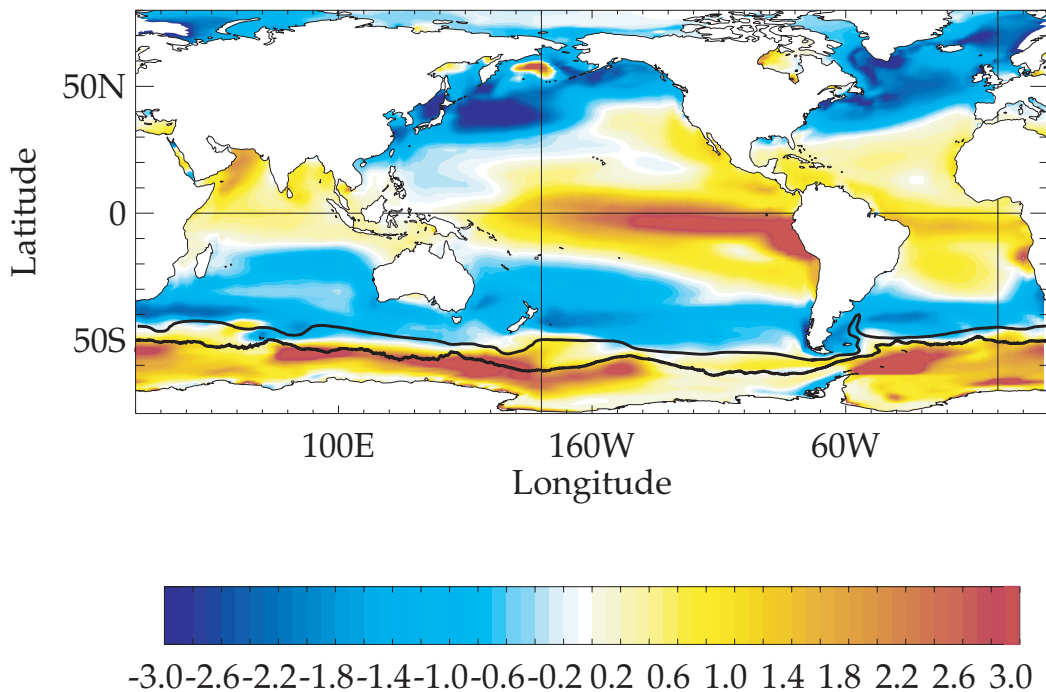


Fig. 4. Annual mean natural air-sea CO₂ fluxes in PISCES-LIM-ORCA2. Here as well as in the following figures, the mean positions of the Polar Front (from Moore et al., 1999) and Sub-antarctic Front (from Belkin and Gordon, 1996) are also reported.

Watermasses and the Southern Ocean carbon cycle

D. Iudicone et al.

Title Page

Abstract Introduction

Conclusions References

Tables Figures

◀ ▶

◀ ▶

Back Close

Full Screen / Esc

Printer-friendly Version

Interactive Discussion



Watermasses and the Southern Ocean carbon cycle

D. Iudicone et al.

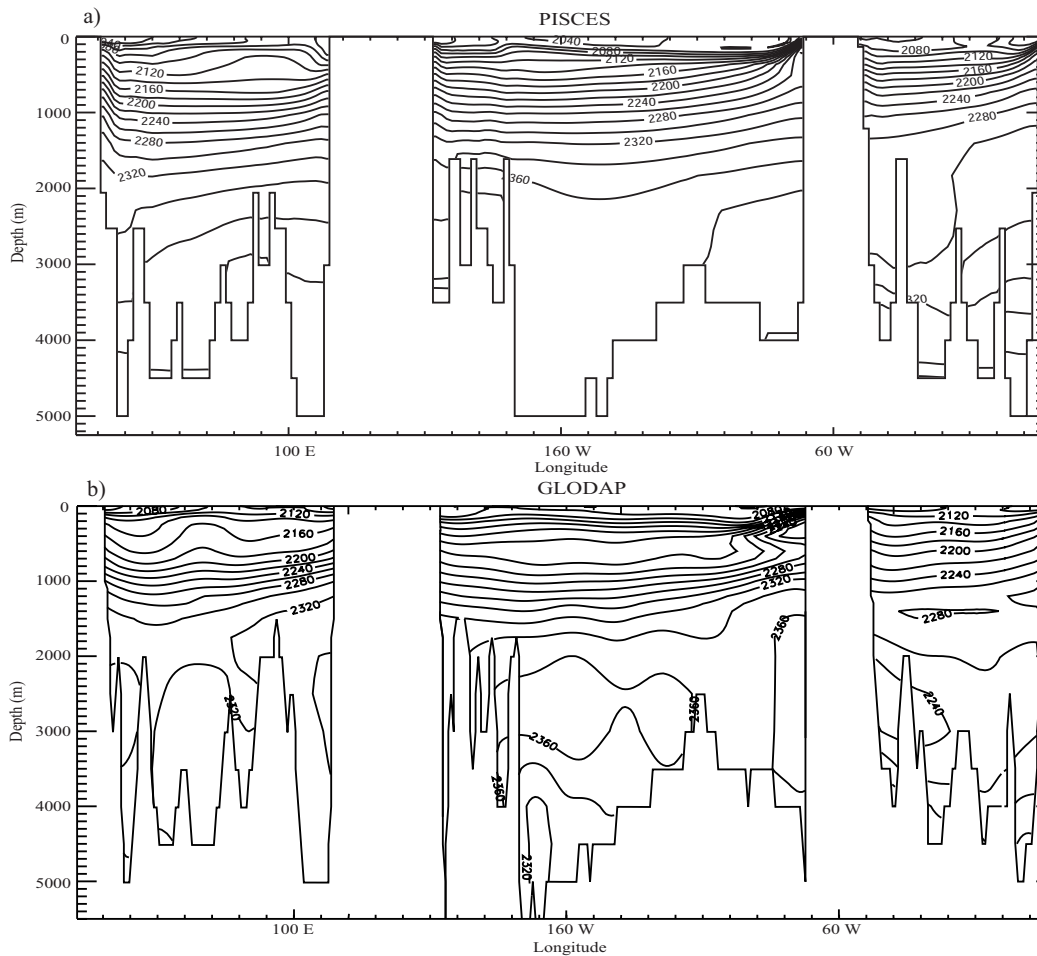


Fig. 5. Annual mean of DIC at 30° S (in $\mu\text{mol/l}$) from GLODAP (lower panel) and PISCES (upper panel), respectively.

Title Page	
Abstract	Introduction
Conclusions	References
Tables	Figures
◀	▶
◀	▶
Back	Close
Full Screen / Esc	
Printer-friendly Version	
Interactive Discussion	

Watermasses and the Southern Ocean carbon cycle

D. Iudicone et al.

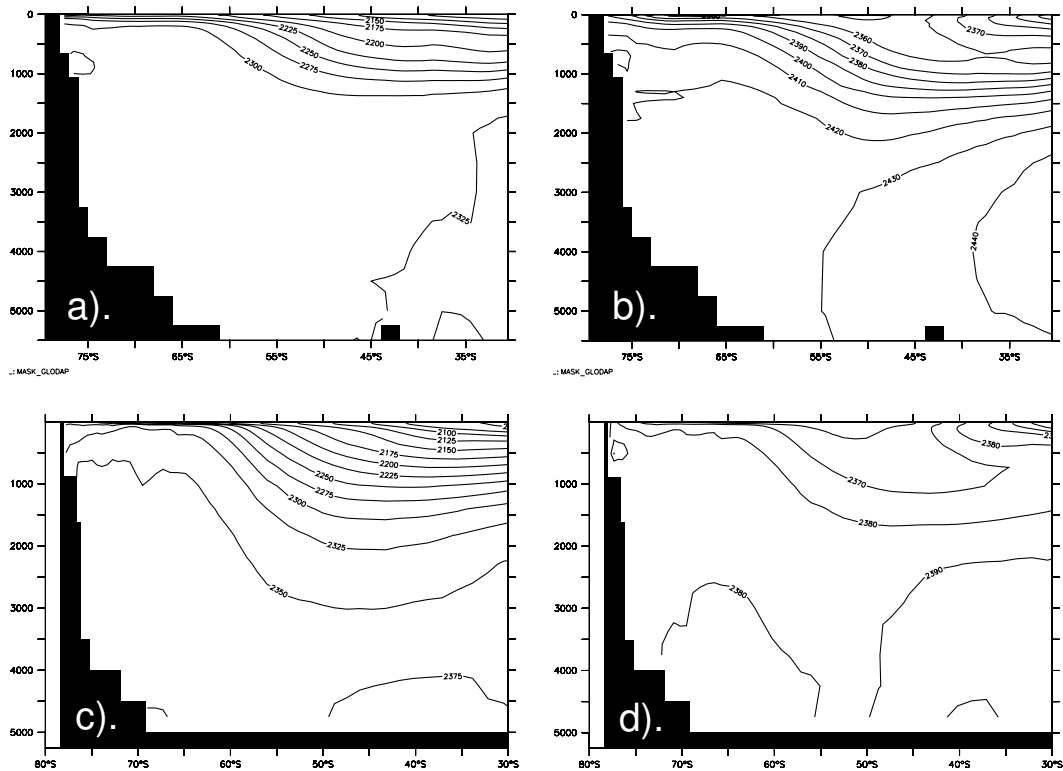


Fig. 6. Annual zonal mean of DIC and alkalinity concentration (in $\mu\text{mol/l}$) from GLODAP (a), (b) and PISCES (c), (d), respectively.

Title Page

Abstract

Introduction

Conclusions

References

Tables

Figures

◀

▶

◀

▶

Back

Close

Full Screen / Esc

Printer-friendly Version

Interactive Discussion



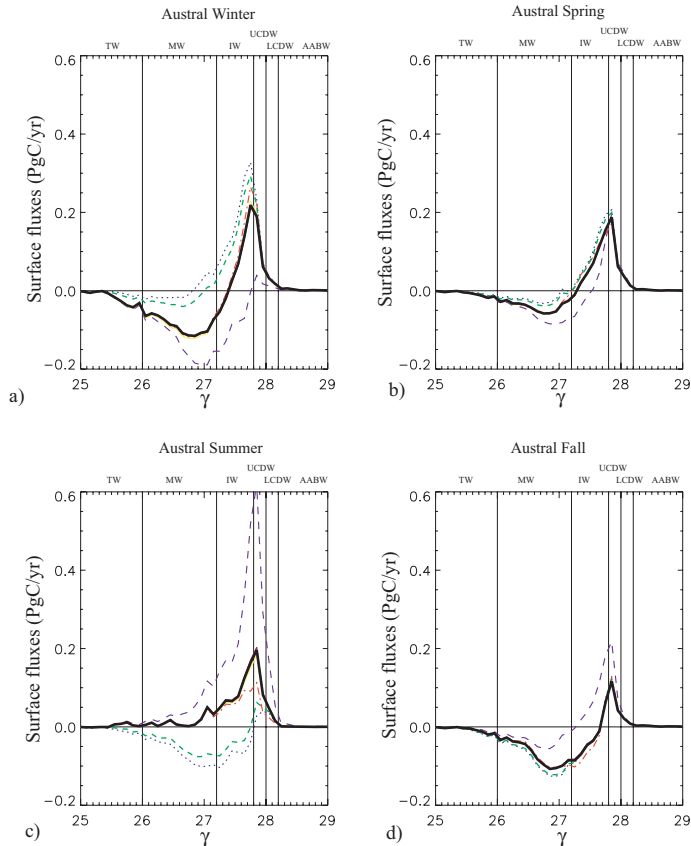


Fig. 7. Density-binned seasonal air-sea CO_2 flux from 30°S to 80°S recomputed in offline (black line) and recomputed removing the effect of DIC (violet dashed line), the effect of temperature (blue dot line), the effect of solubility (green long dashed line), the effect of alkalinity (red dot dashed line), the effect of gas transfer velocity K_w (yellow line) and the effect of salinity (red-purple line) (see Methods).

Watermasses and the Southern Ocean carbon cycle

D. Iudicone et al.

Title Page

Abstract

Introduction

Conclusions

References

Tables

Figures

◀

▶

◀

▶

Back

Close

Full Screen / Esc

Printer-friendly Version

Interactive Discussion



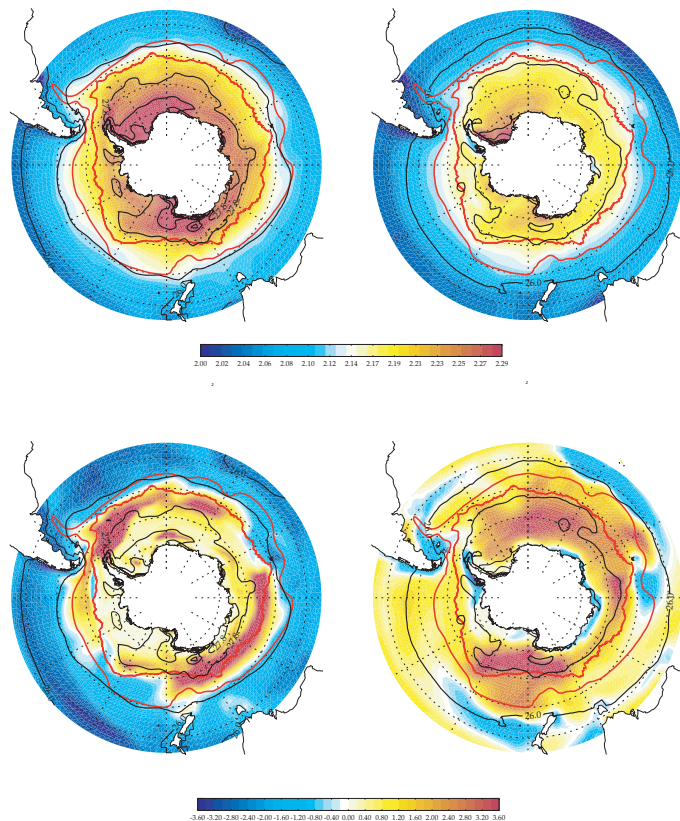


Fig. 8. Upper panels: model surface DIC values (mmol/kg). Left panel: winter values; right panel: summer values. Lower panels: model air-sea CO_2 flux (in $\text{mol/m}^2/\text{yr}$). Left panel: winter values; right panel: summer values. Red contours mark the location of the Southern Ocean fronts: from north to south Subantarctic Front (SAF) and Polar Front (PF). Black contours mark the location of the water masses in winter (for the definition see the Table 1). Negative values indicate a flux toward the ocean.

Watermasses and the Southern Ocean carbon cycle

D. Iudicone et al.

Title Page

Abstract Introduction

Conclusions References

Tables Figures

◀ ▶

◀ ▶

Back Close

Full Screen / Esc

Printer-friendly Version

Interactive Discussion



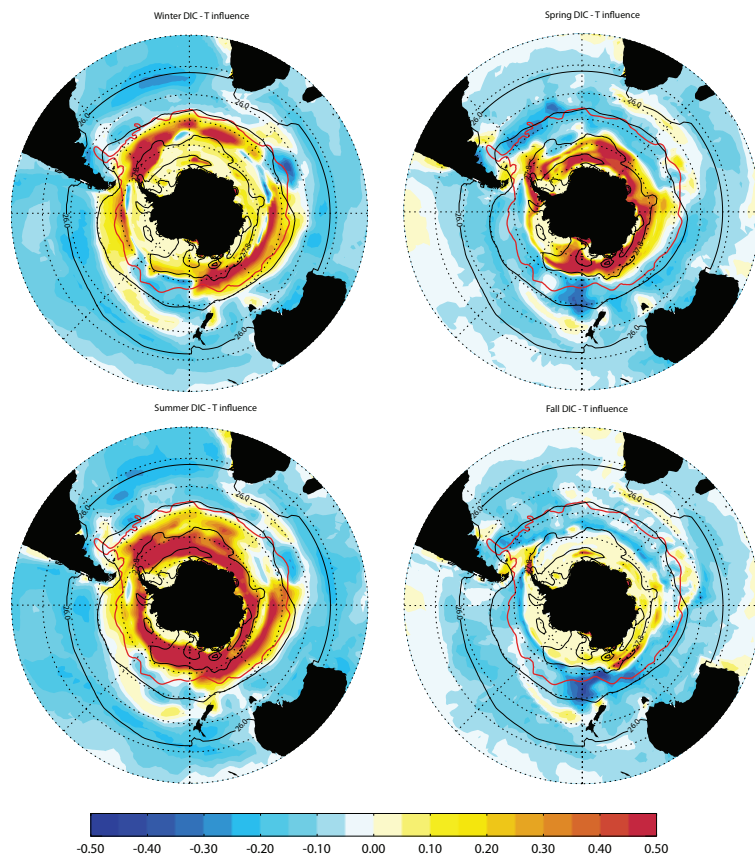


Fig. 9. Difference between the amplitude of the DIC effect and the amplitude the temperature effect in winter, spring, summer and fall (see section on Methods). Negative values correspond to a dominance of the temperature signal. Units are in $\text{mol}/\text{m}^2/\text{yr}$. Black contours mark the location of the water masses in winter, red contour mark the location of the SAF.

Watermasses and the Southern Ocean carbon cycle

D. Iudicone et al.

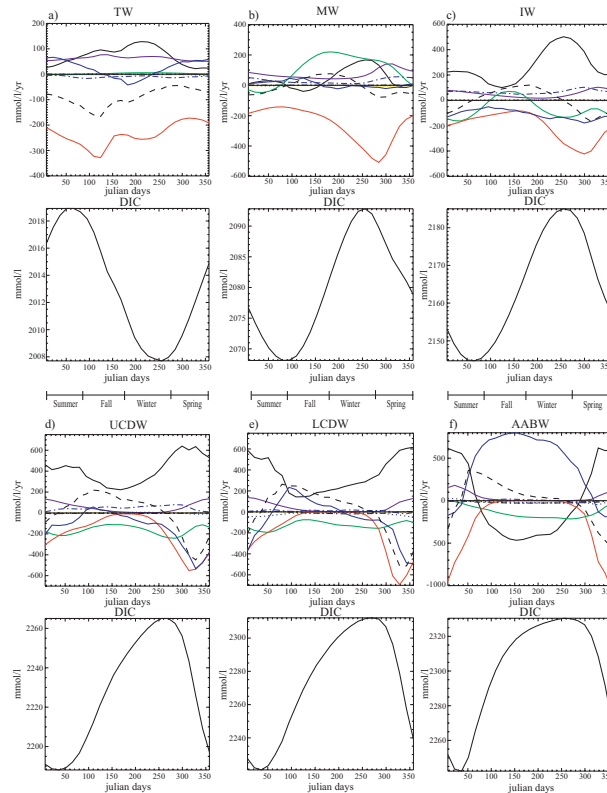


Fig. 10. Annual mean of the physical terms (vertical diffusivity: black line; meridional diffusivity: dot-dashed: black line; zonal diffusivity: dotted black line; vertical advection: blue line; meridional advection: dot-dashed blue line; zonal advection: dotted-dashed line) and biological terms (production: red line; remineralization: violet line; air-sea CO_2 flux: green line) of DIC concentration (in $\mu\text{mol/l/yr}$, plots above) and annual mean of surface DIC concentration (in $\mu\text{mol/l}$, plot below) of the TW (a), of the SAMW (b), of the AAIW (c), of the UCDW (d), of the LCDW (e) and of the AABW (f).

[Title Page](#)
[Abstract](#)
[Introduction](#)
[Conclusions](#)
[References](#)
[Tables](#)
[Figures](#)
[Back](#)
[Close](#)
[Full Screen / Esc](#)
[Printer-friendly Version](#)
[Interactive Discussion](#)


Watermasses and the Southern Ocean carbon cycle

D. Iudicone et al.

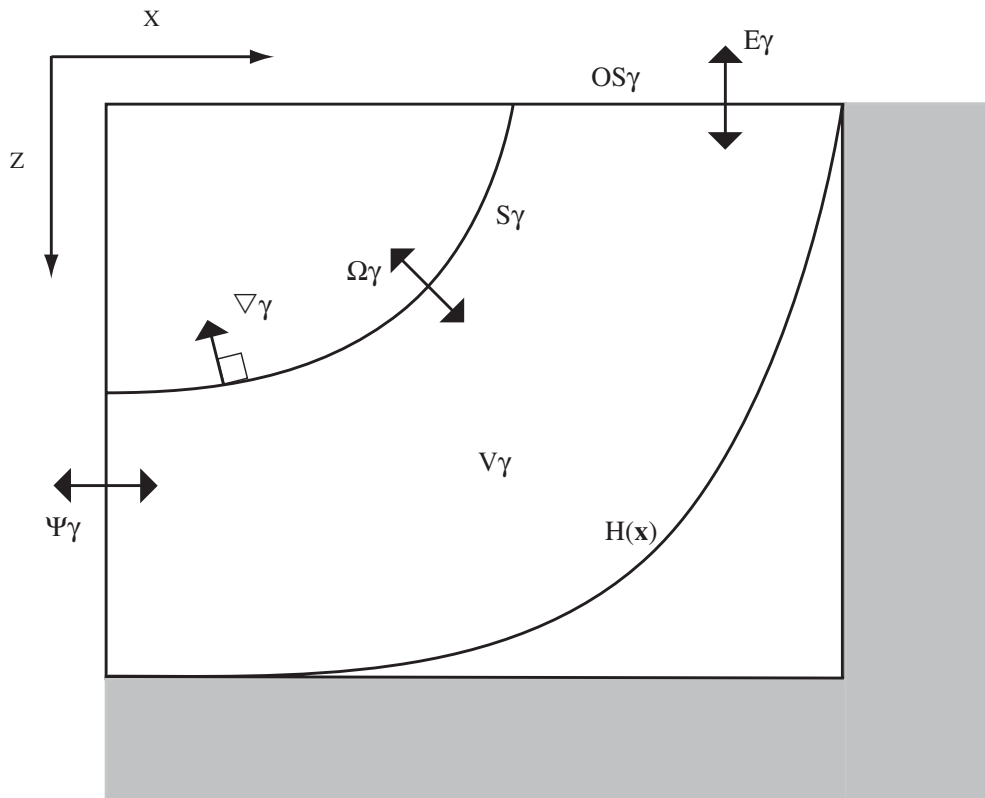


Fig. 11. Sketch of the ideal oceanic basin. Let us consider a limited area of the ocean with an open boundary. We denote S_γ , the surface with neutral density γ over the limited domain; the volume V_γ sandwiched between two surfaces S_γ ; the ocean bottom H ; the ocean surface OS_γ ; Ψ_γ and E_γ the volume fluxes of fluid entering/exiting the domain V_γ across the open boundary and surface, resp.; and Ω_γ , the total volume flux across the S_γ (i.e. the dianeutral volume flux). The sign convention is that all the fluxes are positive if entering V_γ .

Title Page

Abstract

Introduction

Conclusions

References

Tables

Figures

◀

▶

◀

▶

Back

Close

Full Screen / Esc

Printer-friendly Version

Interactive Discussion



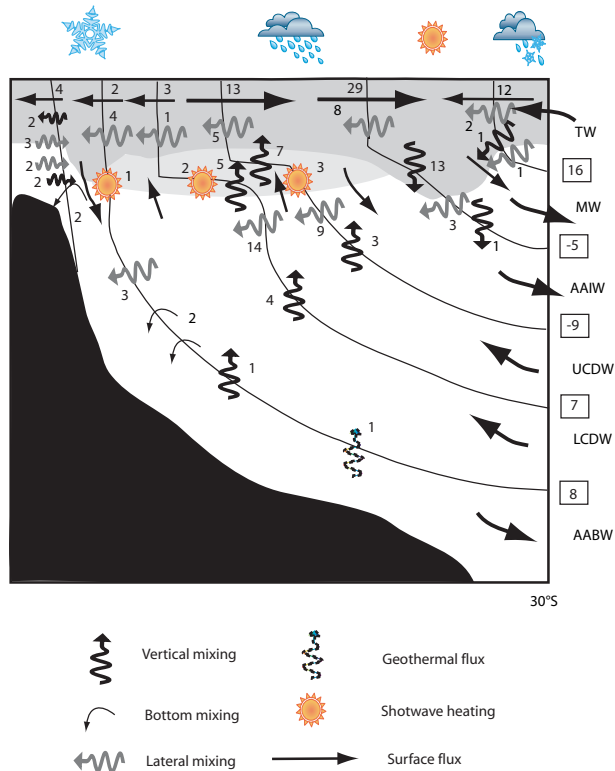


Fig. 12. Sketch of the principal model watermass transformations in the model (from Iudicone et al., 2008a, Copyright by American Meteorological Society). Units are in Sv. The DIC transport due to diapycnal fluxes is very similar and, in fact, to a good approximation, 1 PgC/y corresponds to 0.8 Sv. Numbers on the right refer to the net diapycnal volume transport (positive values correspond to transport toward larger densities). The dark shaded region is the region of annual maximum mixed layer depth while the light shaded region is the stratified region impacted by the solar heating. Numbers are rounded off and thus the net budgets are within 1 Sv the sum of the components. For a discussion of assumptions made in the computations in Iudicone et al. (2008a).

Watermasses and the Southern Ocean carbon cycle

D. Iudicone et al.

Title Page

Abstract

Introduction

Conclusions

References

Tables

Figures

◀

▶

◀

▶

Back

Close

Full Screen / Esc

Printer-friendly Version

Interactive Discussion



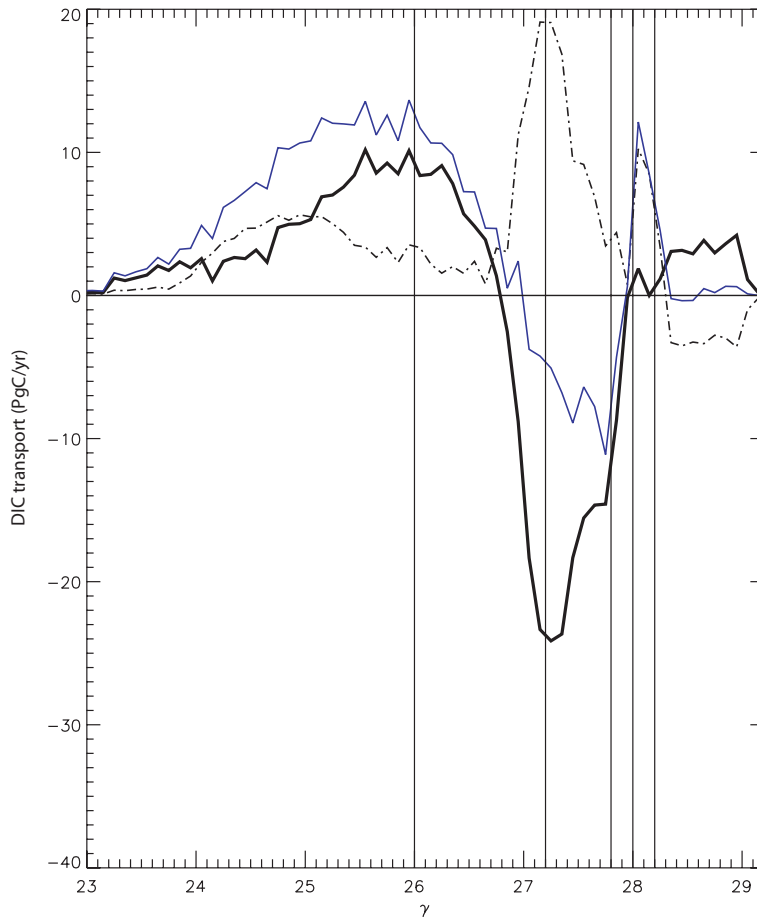


Fig. 13. Dianeutral transport $\Phi_{\gamma}(\Theta=30^{\circ}\text{S})$ of DIC (PgC/yr) per water masses. Continuous thin line: net transport; Dot-dashed line; transport due to mixing processes; continuous thick line: transport due to surface buoyancy fluxes. The vertical line delimitate the water mass boundaries.

Watermasses and the Southern Ocean carbon cycle

D. Iudicone et al.

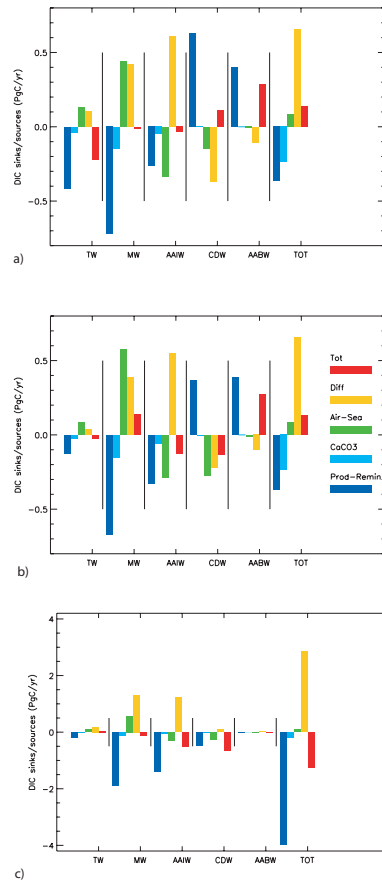


Fig. 14. Budget (PgC/yr) per water masses of the sink/sources of DIC (Eq. 2). **(a)** Values for the full case; **(b)** Values for the case of using the winter isopycnals as water masses boundaries; **(c)** The same as in (b) but for the upper 120 m.

Watermasses and the Southern Ocean carbon cycle

D. Iudicone et al.

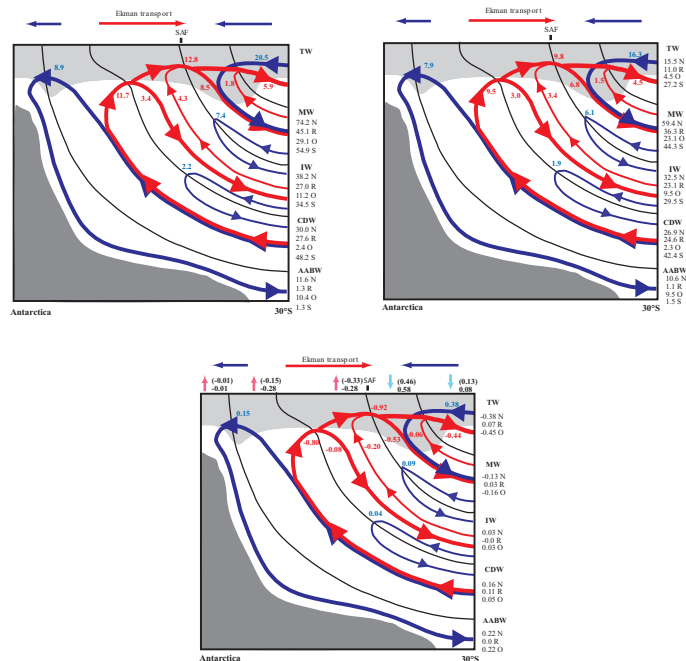


Fig. 15. A sketch of the overturning circulation in the Southern Ocean in the ice-ocean model with the main watermass transformations. For sake of simplicity, the recirculation is not represented as well as the transformation less important, the UCDW and LCDW has been merged into a unique CDW layer. The numbers along the vertical column correspond to: the total northward transport (N), the component of the northward transport that recirculated within the isopycnal layer (R), the component of the northward transport water at the origin was in a different density class (overturning; O) and total southward transport (S). Upper left panel: Volume transport (Sv). Upper right panel: DIC transport (PgC/yr) associated to the different branches of the overturning. The numbers correspond to the gain (positive values) or loss (negative values) of DIC. Lower panel: DIC sources/sinks associated to the different branches of the overturning circulation (PgC/yr). The numbers along the vertical column correspond to: the gain/loss of DIC when the water mass leaves the Southern Ocean at 30° S (N), the gain/loss of DIC for the recirculation (R); and the gain/loss of DIC for the overturning. At the surface there are the air-sea CO₂ fluxes (Pg C/yr) for each water mass computed considering the winter density while in parenthesis are the flux computed without considering the winter density. The light blue arrows indicate the fluxes toward the ocean while the magenta arrows indicate the fluxes toward the atmosphere.

Title Page

Abstract

Introduction

Conclusions

References

Tables

Figures

◀

▶

◀

▶

Back

Close

Full Screen / Esc

Printer-friendly Version

Interactive Discussion